CHAPTER 4

Study of Conventional and Rubber-Assisted Forming Processes

4.1 Introduction

The design and development of RBSH set up has been discussed in chapter3. This set up is used to carry out to a number of experiments to evaluate the formability of rubber based forming process. The experiments are primarily focussed on comparative formability study of Conventional forming and Rubber assisted forming. The formability has been evaluated in terms of percentage thinning, plastic strains, developed stresses and distortion of microstructure grains. The experiments are carried out for both 'Shallow forming' and 'Deep drawing' applications. The experimental details and formability analysis for each case has been discussed in this chapter.

4.2 For height to diameter ratio less than 0.5 (Shallow Forming)

4.2.1 Study for Cup made of SS-304

Die Design and Component Description for Polyurethane Rubber Trial

It was established using FEM simulation as discussed in Chapter 5 that the stress developed in 'Rubber based sheet hydroforming process' was considerably less than the stress developed in Conventional Drawing process. In order to verify the same, Conventional Dies assembly and 'Rubber Based Dies' Assembly are designed and fabricated for a axisymmetric component. The component is made up of Stainless Steel 304 and having thickness of 1.5mm. The trials are conducted to draw the

same component in these two different set ups. The CAD model of the component is shown in Figure 4.1.

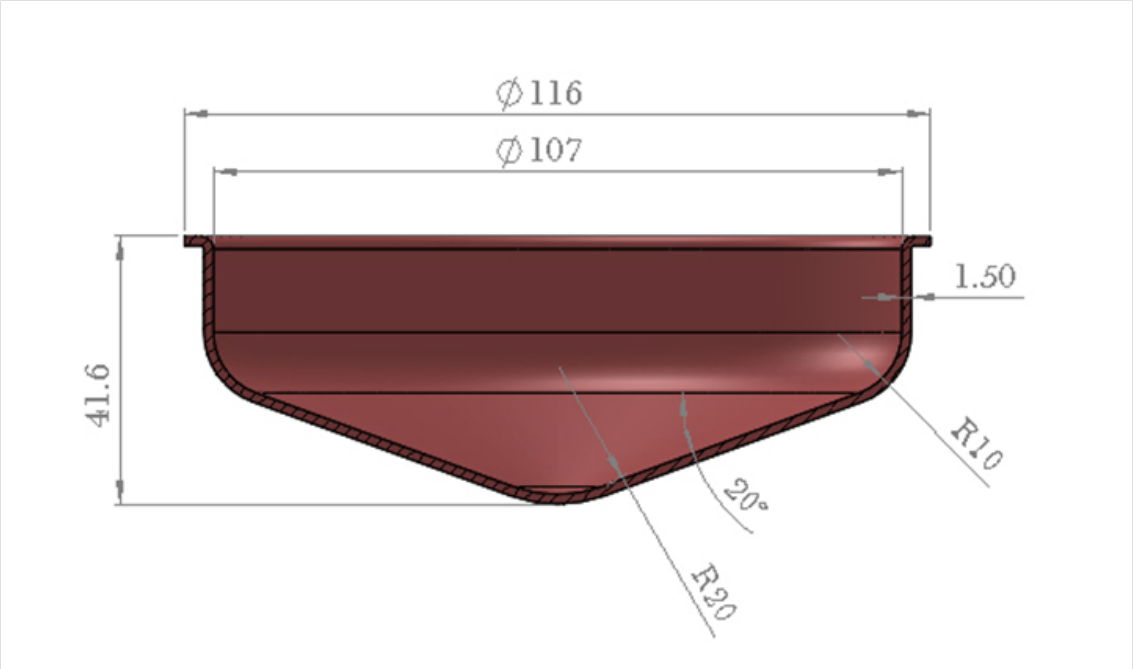

Figure 4.1: 3D CAD model of the trial component (SS304)

In figure 4.2, the Die design for a conventional drawing process is shown. The assembly consists of a Die, Punch and Blank holder (not shown here). In conventional Drawing process, there is a Solid Die and Solid Punch. The clearance between die and punch is kept approximately equal to the thickness of the component. Here the component thickness is 1.5 mm, hence the clearance is also 1.5 mm. The Die assembly for Rubber-based drawing process is slightly different from the above assembly. The details are shown in figure 4.3. The assembly is very similar to 'Verson-Hydroform' set up. In present case, set-up has been designed without any hydraulic pressure.

In Rubber Based Drawing process, there is Die block instead of Solid Die. Below the Die block, Rubber Sheet (Polyurathene etc) can be used to support the component at the later stage of drawing. The Hydraulic pressure is also used to generate required compressive stress and to improve the formability of the process. In present case polyurethane sheet of thickness 6mm has been used.

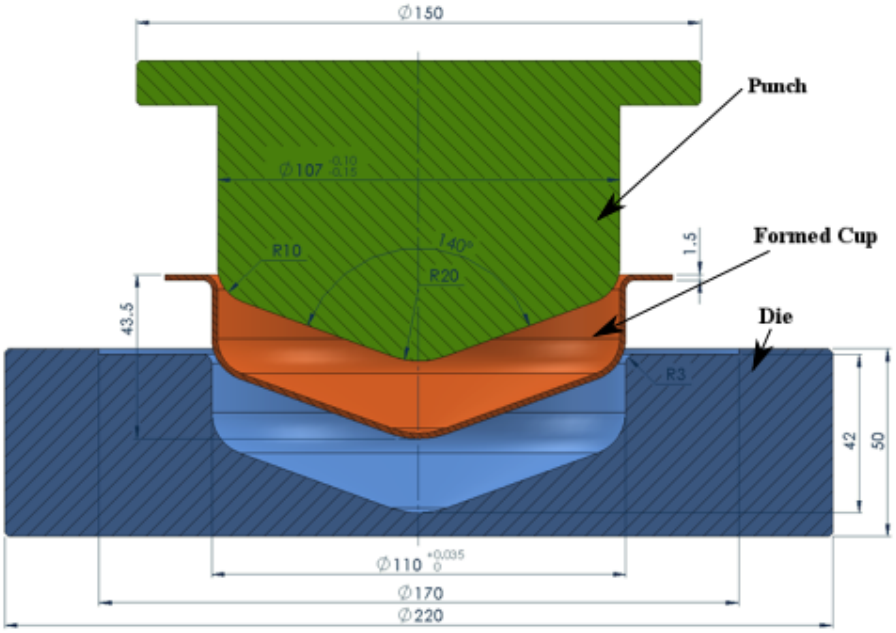

Figure 4.2: CAD model of Tool assembly for conventional Drawing Process

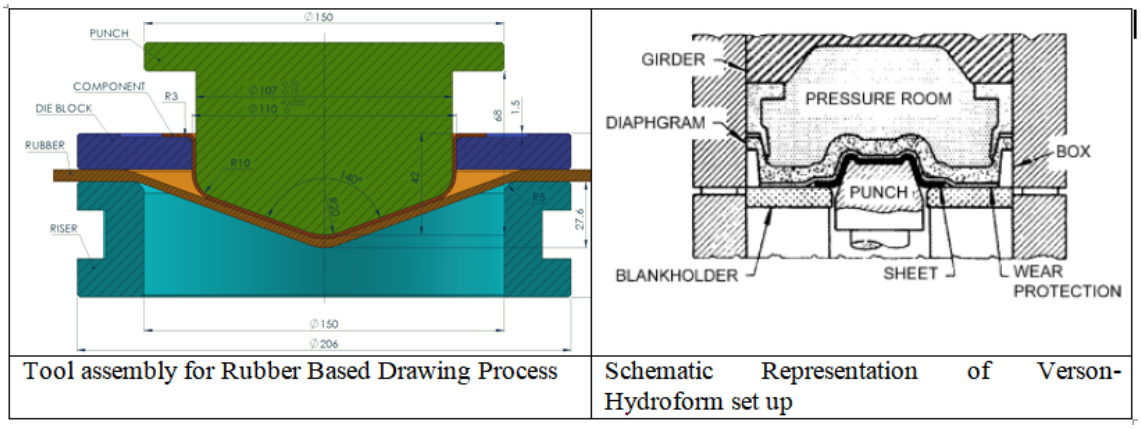

Figure 4.3: CAD model of Tool assembly for Rubber Based Drawing Process

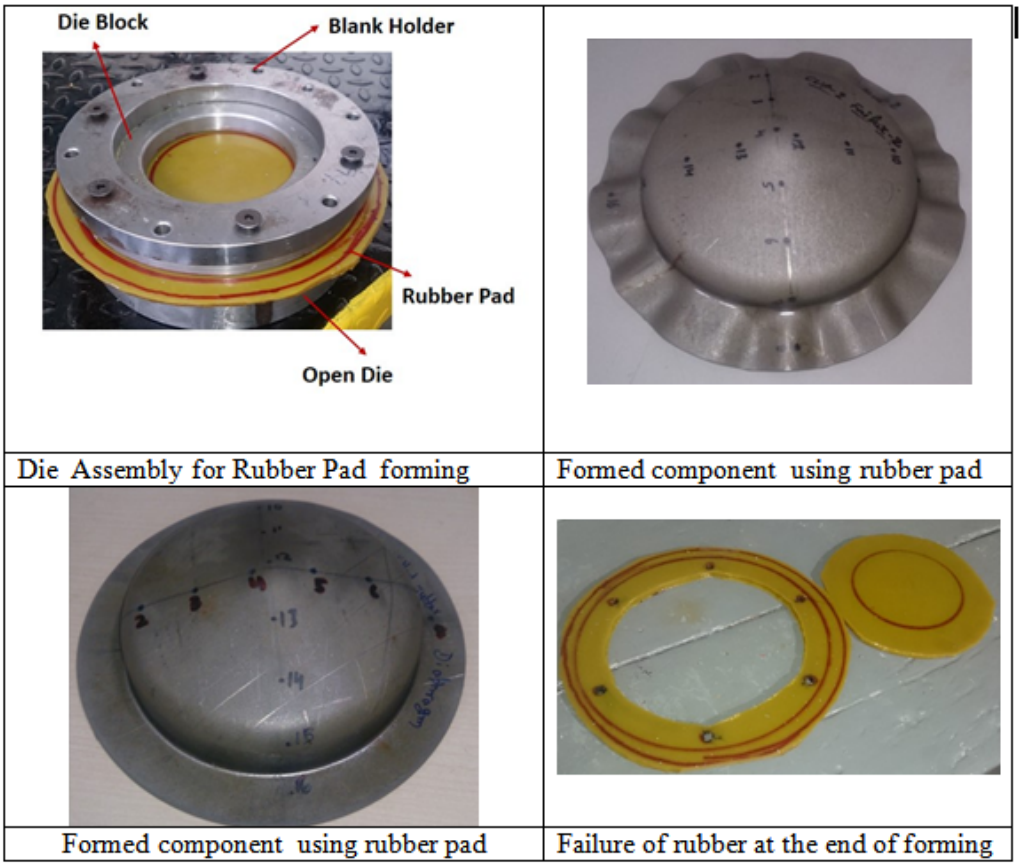

Figure 4.4: Die assembly and formed components

Fabrication of Dies and 'forming' of component

The Dies are fabricated as per CAD models shown in figure 4.2 and figure 4.3. In figure 4.4 formed components and dies assemblies are shown. As shown in figure4.4, the components are formed both using rubber pad and without rubber pad. Rubber pad is having the thickness of 6 mm and it failed at the end of forming.

Comparison of stresses developed after forming in both the processes

The Stresses are measured in the both the sheets before forming and after forming. The stresses developed after forming are measured and evaluated to establish the severity of stress in both the processes. 12 points are marked on the blank and principle stresses are measured before forming. The principle stresses are measured again at these points again after forming. Figure 4.5 is showing these reference points.

The principle stresses are measured using XRD- stress measurement equipment.

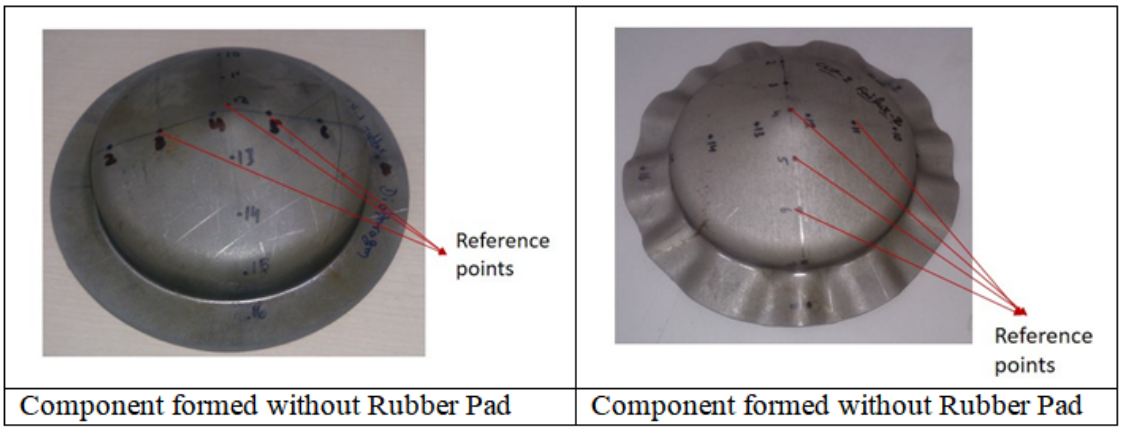

Figure 4.5: Reference points to measure stress

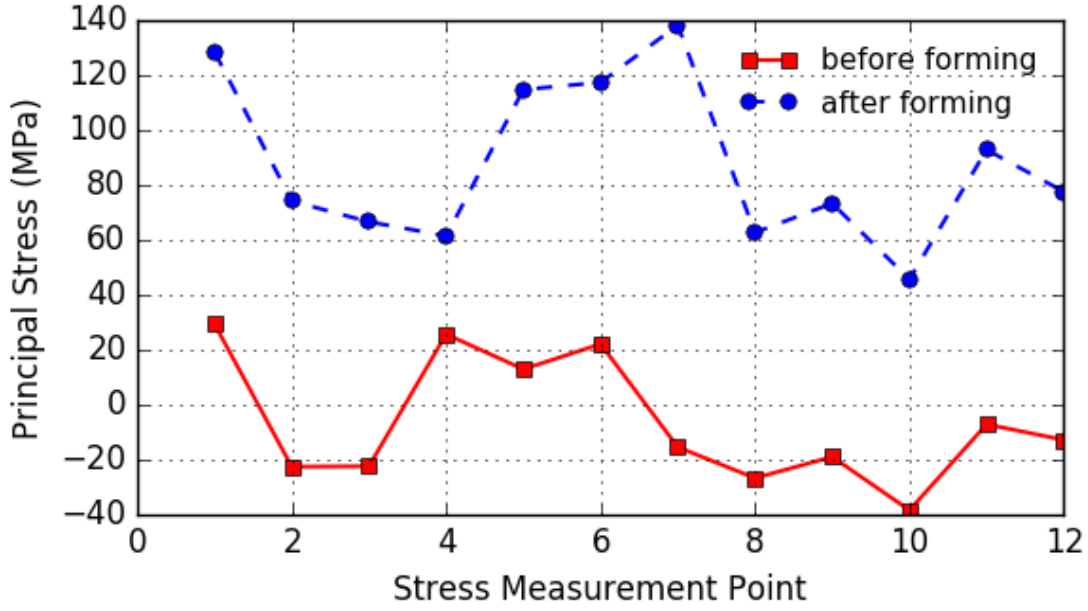

Figure 4.6: Max Principle Stress Variation in Component formed without Rubber Pad

It works on the principle of X-ray diffraction and gives out in terms of principle stresses. The comparison of Stresses in the component formed without rubber pad are shown in Figure 4.7. In Figure 4.8 the variation in Max Principle stresses in the component formed using Rubber Pad is shown. The following points can be inferred from both the plots

- There is development of tensile stresses in both the cases which is expected in case of deep drawing.
- Max Tensile stress was developed near the point adjacent to the tip of the

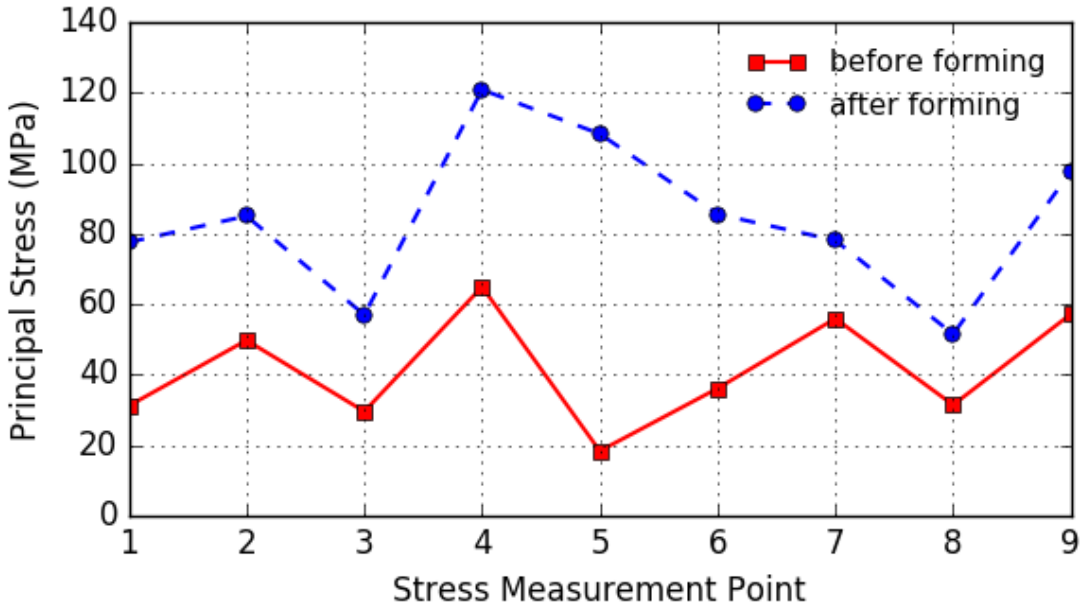

Figure 4.7: Max Principle Stress Variation in Component formed with Rubber Pad

component.

- Max principle stress variation in 1st case (without rubber forming) is at point 7 and is 160 MPa approx.
- Max principle stress variation in 2nd case (with rubber forming) is at point 5 and is 90 MPa approx.
- Hence the rise in tensile stress is less in Rubber pad forming.
- The compressive stress generated by Rubber pad is playing major role in restricting the growth of tensile stress.

Natural Rubber for next trials

As Polyurethane rubber failed in previous trial, the experiemnt is repeated with Natural rubber Cis1,4 Polyisoprene with minor die modifications. The uniqueness of natural rubber lies in its physical properties of **extensibility and toughness**, summarized by its ability to be stretched repeatedly to seven or eight times its original length. In the absence of tensile (stretching) stress, the polymer chains assume an amorphous, or disordered, arrangement. On being stretched, however, the molecules readily align into an ordered crystalline arrangement. Crystallinity lends greater strength to the material, so natural rubber is considered to be "self-reinforcing"[8]. The rubber pad of thickness 3 mm has been manufactured. The polymer chain is shown in figure 4.8.

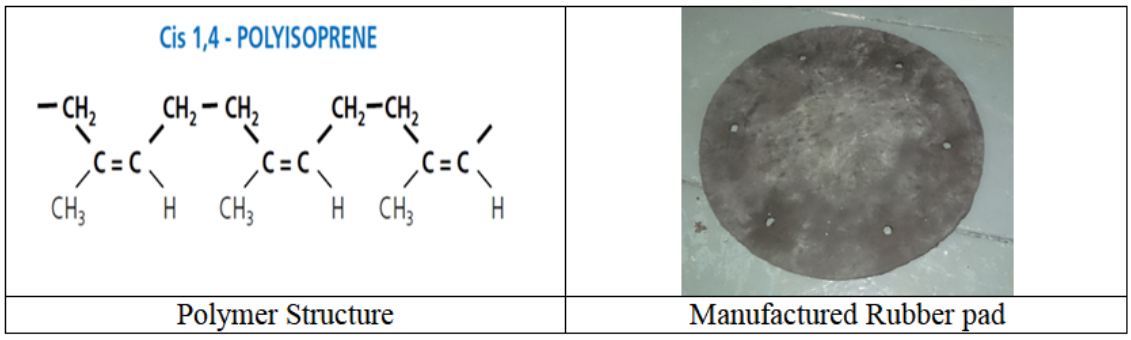

Figure 4.8: Natural Rubber

Die Assembly for Natural Rubber Trials

Conventional Dies assembly and 'Rubber Based Dies' Assembly are designed and fabricated for a axisymmetric component. The component made up of Stainless Steel 304 and Pure Copper having thickness of 0.8 mm are used for trials. The Die assemblies are shown in Figure 4.9

In Rubber Based Forming process, Solid die is replaced with Die block. Below the Die block, Rubber Sheet (Rubber Sheet etc) can be used to support the component at the later stage of drawing. The Hydraulic pressure is generally used to generate required compressive stress and to improve the formability of the process. However, like in previous case hydraulic pressure is not used in this trial. Natural Rubber sheet of thickness 3 mm has been used.

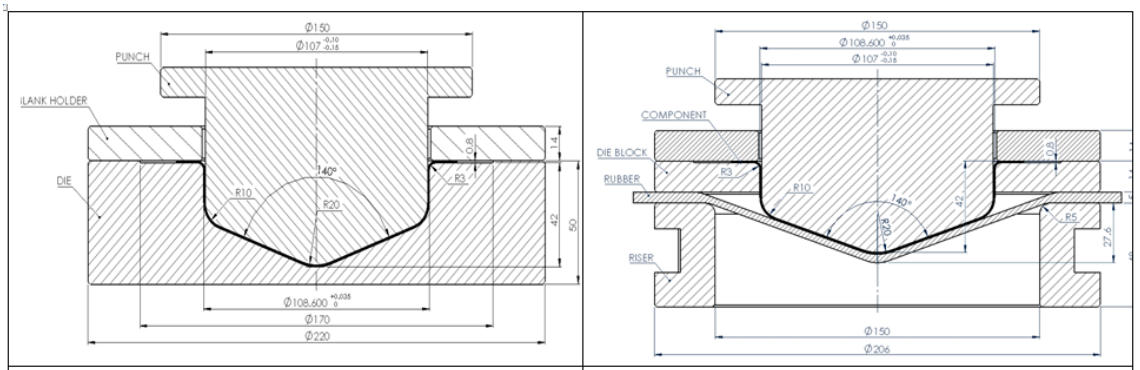

Tool assembly for Conventional Drawing Process | Tool assembly for Rubber Based Drawing Process

Figure 4.9: Tool Assemblies for both the Processes (SS304)

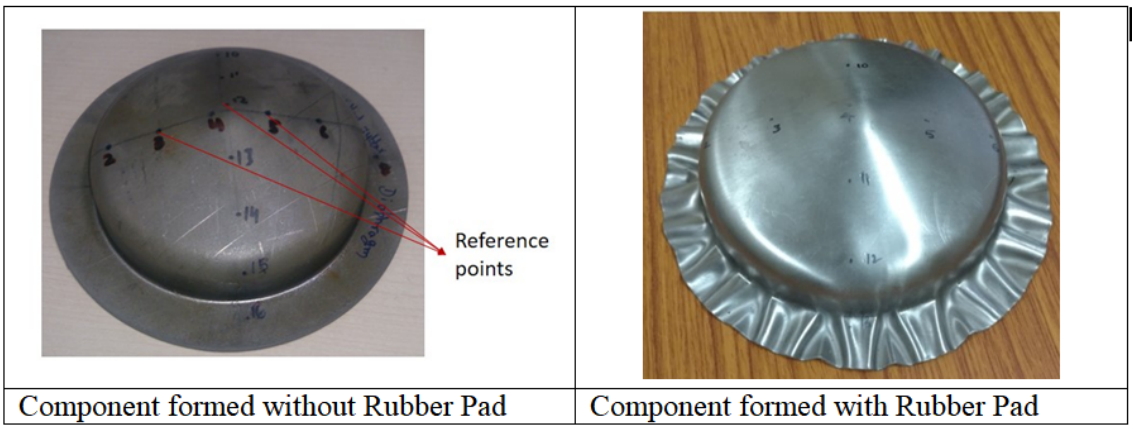

Component formed without Rubber Pad | Component formed with Rubber Pad

Figure 4.10: Components formed using both Processes (SS304)

Comparison of Hardness Value for both the Processes (With Rubber and without Rubber)

The trial component made up of SS304 is drawn using both processes. In first process, Solid Die Cavity is used to draw the component, whereas in 2nd process, Rubber supported the drawing operation. All the blanks were annealed to relieve all the residual stresses for better comparison of the processes. The formed components are shown in figure 4.10. To start with, 12 points are marked on the blanks and hardness values were noted. Then on the same point, hardness vales are again measured after forming. The measured hardness values in BHN are given in table 4.1.

The comparison in “Increase of Hardness" is presented in figure 4.11. The maximum increase in hardness for ‘rubber assisted’ and ‘without rubber’ forming is 248

Table 4.1: Hardness measured using ECHO TIP for Stainless Steel (SS-304)

Hardness values of Stainless Steel 304 in BHN				
Process	**S. No**	**Before Drawing**	**After Drawing**	**Difference**
With Rubber	1	169	NM[a]	NM
	2	168	331	163
	3	169	405	236
	4	176	424	248
	5	183	365	182
	6	172	364	192
	7	0	NM	NM
	8	175	NM	NM
	9	186	338	152
	10	173	355	182
	11	175	415	240
	12	180	317	137
	13	169	NM	NM
Without Rubber	1	174	NM	NM
	2	178	495	317
	3	163	540	377
	4	173	444	271
	5	145	487	342
	6	173	435	262
	7	170	NM	NM
	8	176	NM	NM
	9	162	479	317
	10	176	500	324
	11	171	500	329
	12	173	464	291
	13	177	NM	NM

[a]Not measured

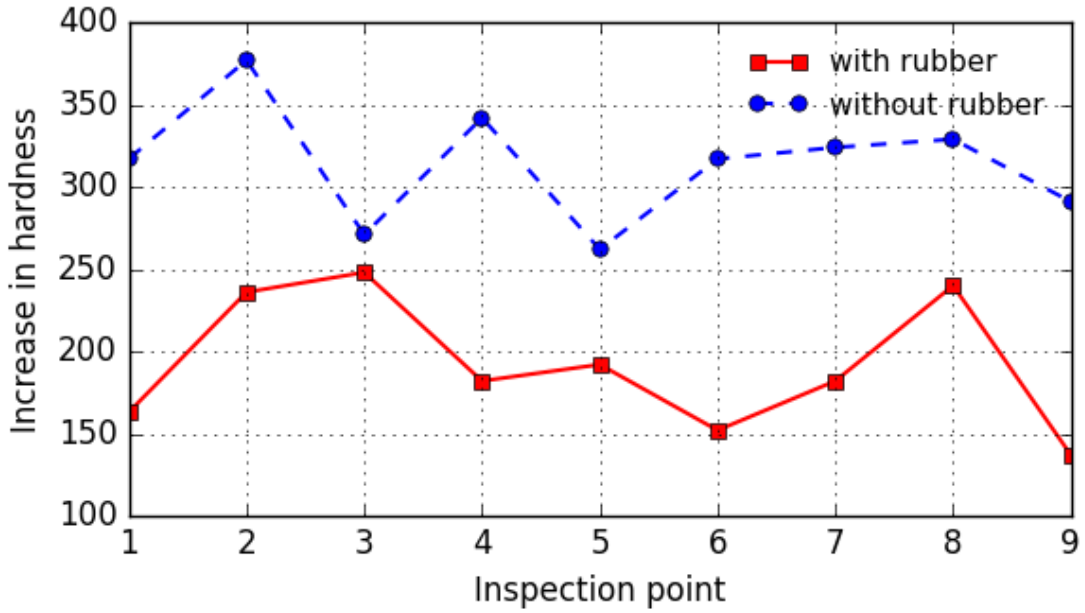

Figure 4.11: Increase in Bulk Hardness Comparison (SS304)

BHN and 377 BHN respectively. Since, Hardness is proportional to Stress generated in the component, it can be inferred that rubber based process generated less stress in the component. This has been further verified through microstructure analysis.

Microstructure Analysis and Comparison

Samples are prepared using the 10mm width of the component along the profile. The representation of the sample is shown in figure 4.12. The samples are prepared as per ASTM E3-11 standard [67]. The analysis is carried to study the variation in microstructure size, zone of twinning and micro-hardness variation. The samples are shown in figure 4.13. The microstructure grain analysis was carried out as per ASTM E112 [68].

The microstructure was captured at 4 locations in both the components as shown in figure 4.14. The microstructures at all the 4 locations for rubber-assisted process is presented in figure 4.15. It is clearly evident that all 4 microstructures are more or less same and there is no significant pattern of grain distortion. It can be inferred that the strain induced in the component is more or less uniform. Figure 4.16 shows the microstructures for “Without Rubber Process". Flow lines are clearly visible and even grain patterns are not uniform. Hence it can be inferred that the deformation

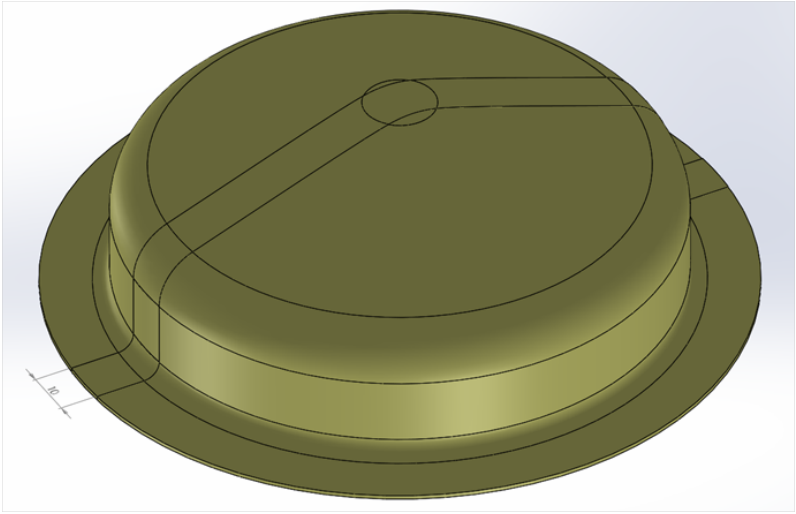

Figure 4.12: 3D model for Sample location (SS304)

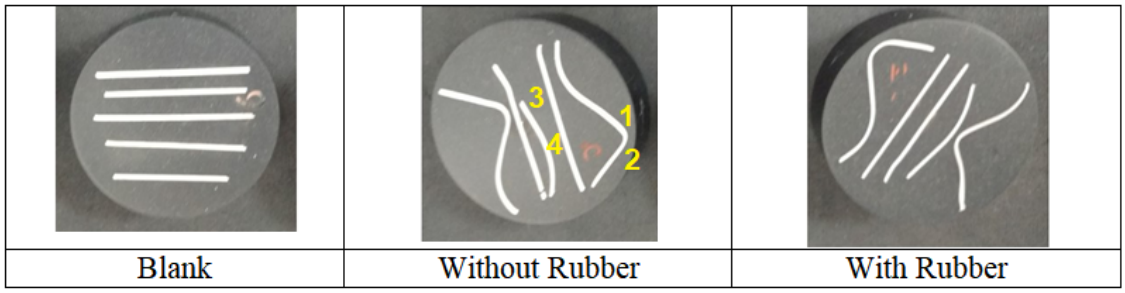

Figure 4.13: Samples for Microstructure (SS304)

in this case in not uniform and more severe.

The comparison of microstructures at location 2 (location experiencing maximum deformation) is presented in figure 4.17 . The flow lines are very dense and clearly visible in “without rubber process". Also the grains are slightly more distorted in this case. Whereas “Rubber assisted Process" has very fine flow lines which indicate that deformation in this case is significantly less.

4.2.2 Study for Cup made of Pure Copper

Die Design and Component description

In order to verify the effect of rubber diaphragm on other material, pure copper instead of SS-304 is selected for this experiment. Die design for rubber forming and conventional forming remains same, as of trail with SS-304. The components made up of pure Copper having thickness of 0.8mm is used for trials. The die assemblies

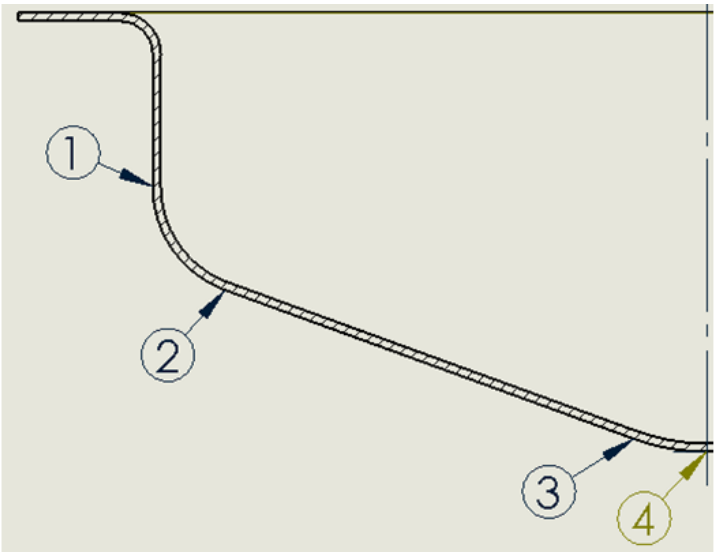

Figure 4.14: Locations for Microstructure analysis (SS304)

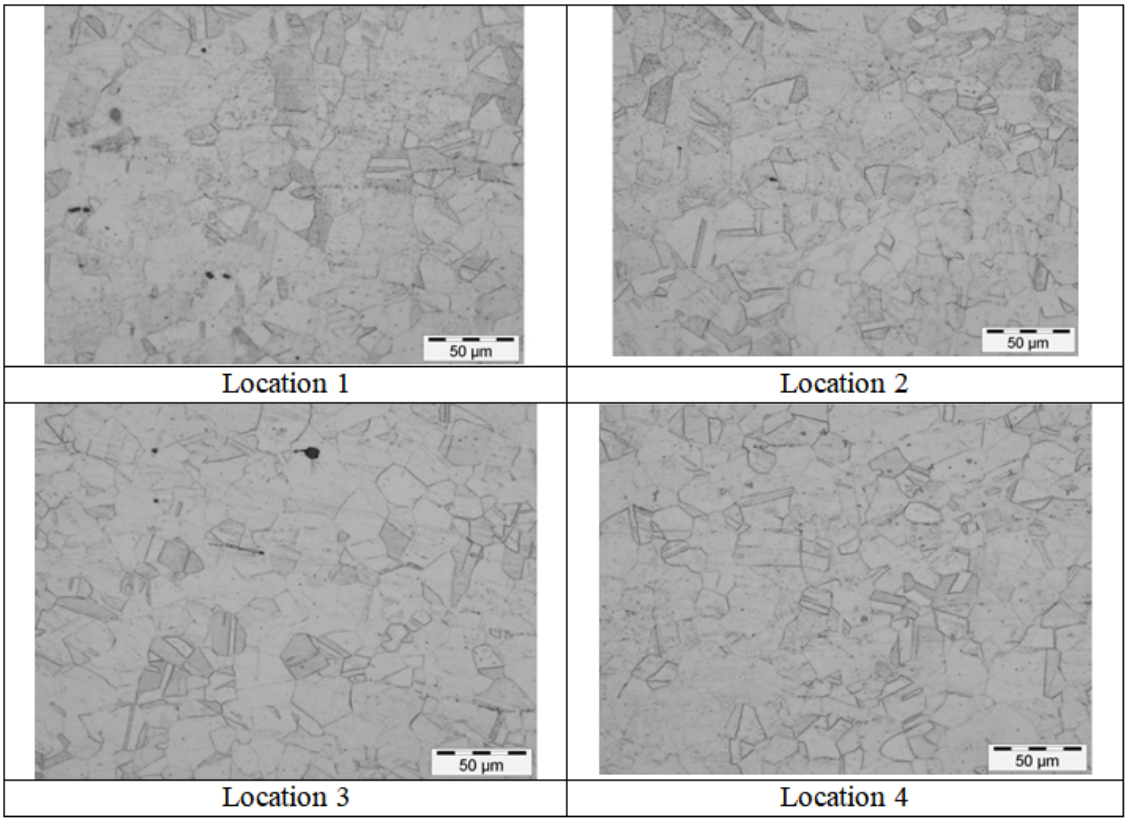

Figure 4.15: Microstructures (Rubber Assisted Process (SS304))

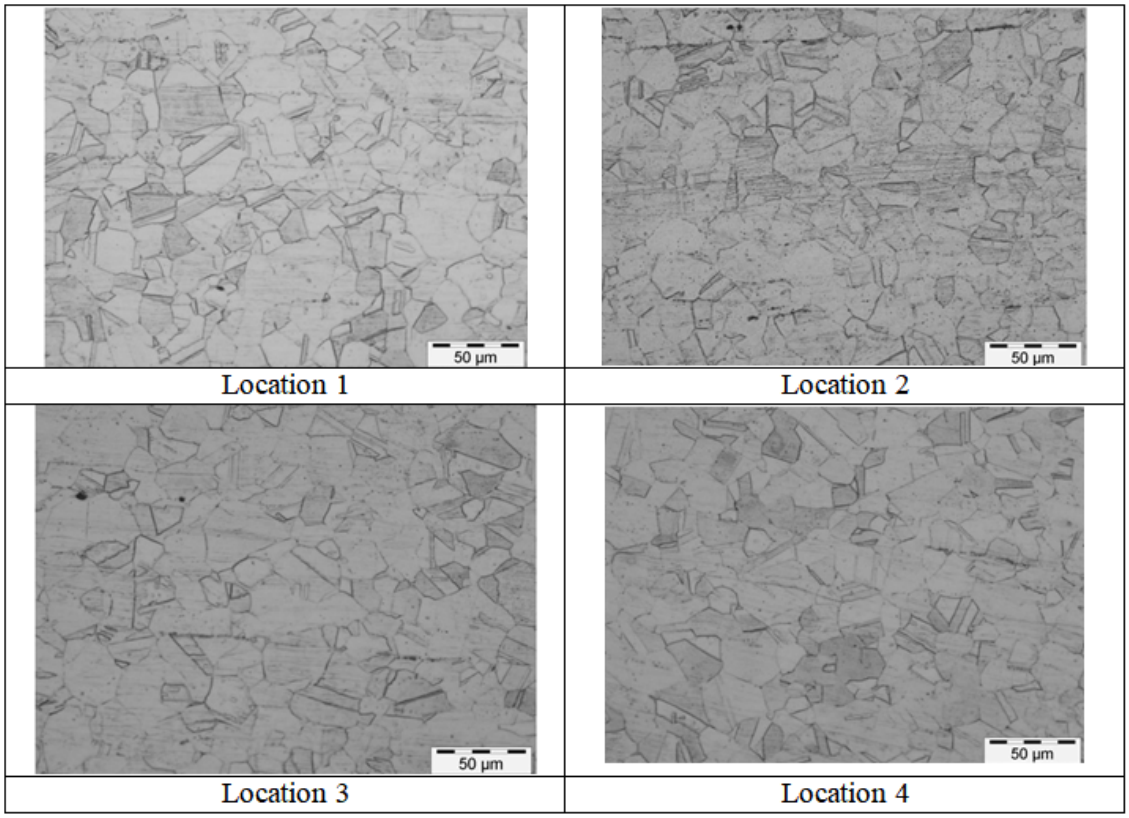

Figure 4.16: Microstructures (Without Rubber Process)

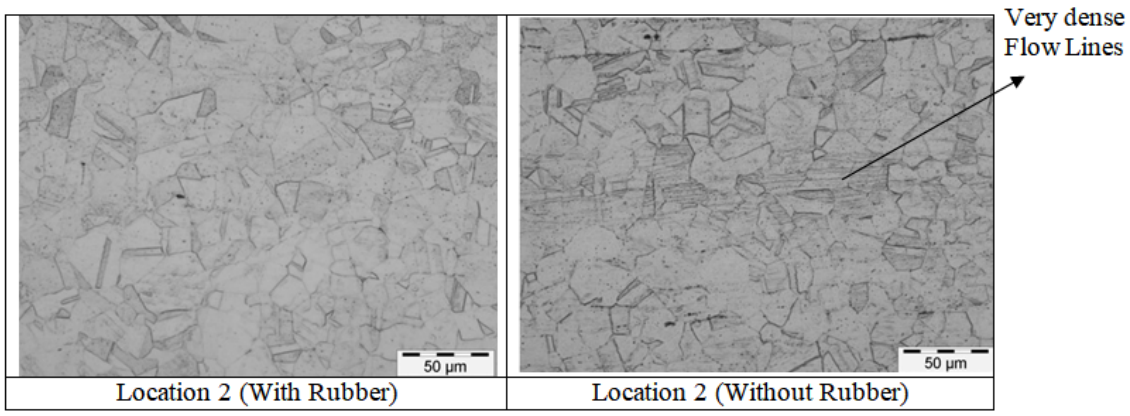

Figure 4.17: Comparison of Microstructures (SS304)

are shown in Figure 4.18. In present case also, Natural Rubber sheet of thickness 3 mm has been used.

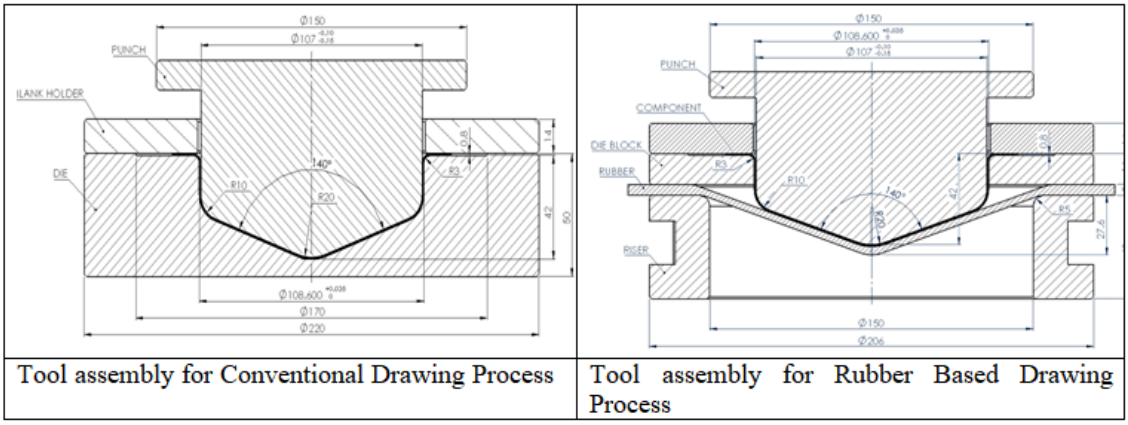

Tool assembly for Conventional Drawing Process | Tool assembly for Rubber Based Drawing Process

Figure 4.18: Tool Assemblies for both the Processes (pure Copper)

Comparison of Hardness Value for both the Processes (With Rubber and without Rubber

The trial component made up of pure copper was fabricated using both processes. In first process, Solid Die Cavity was used to draw the component, whereas in 2nd process, Rubber supported the drawing operation. All the blanks were annealed to relieve all the residual stresses and better comparison of the processes. The formed components are shown in figure 4.19.

To start with, 12 points are marked again on the blanks and hardness values (in BHN) are noted. Then on the same point, hardness vales are again measured after forming. The measured hardness values in BHN are given in table 4.2.

The comparison in “Increase of Hardness" is presented in figure 4.20. The max-

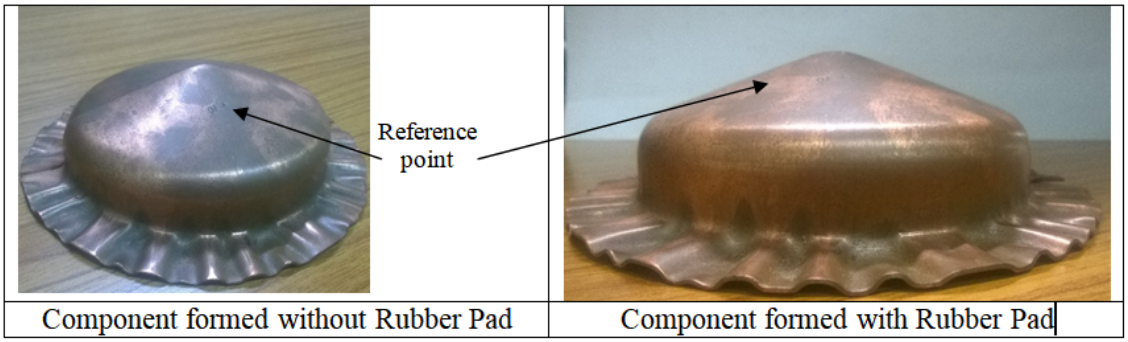

Component formed without Rubber Pad | Component formed with Rubber Pad

Figure 4.19: Components formed using both Processes (pure Copper)

Table 4.2: Hardness measured using ECHOTIP for Pure Copper

Hardness values of Pure Copper in BHN				
Process	**S. No**	**Before Drawing**	**After Drawing**	**Difference**
With Rubber	1	71	NM	NM
	2	72	160	88
	3	70	135	65
	4	69	210	141
	5	70	210	140
	6	72	105	33
	7	68	NM[a]	NM
	8	70	NM	NM
	9	70	166	96
	10	72	205	133
	11	72	175	103
	12	69	113	44
	13	68	0	NM
Without Rubber	1	65	NM	NM
	2	65	204	139
	3	71	230	159
	4	67	216	149
	5	74	234	160
	6	72	163	91
	7	70	NM	NM
	8	69	NM	NM
	9	67	NM	NM
	10	69	180	111
	11	69	248	179
	12	66	184	118
	13	69	NM	NM

[a]Not measured

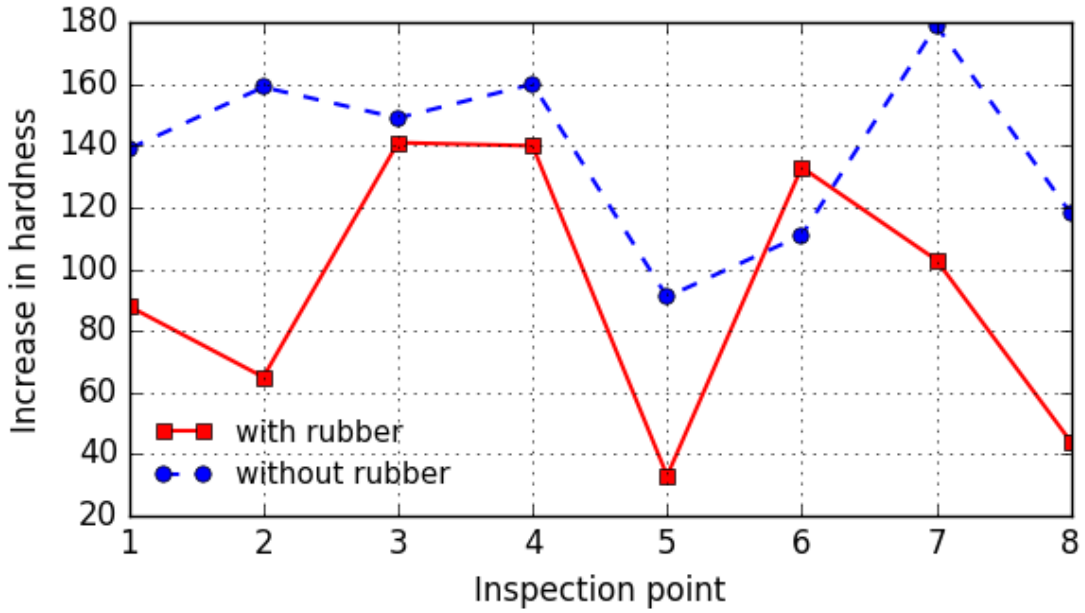

Figure 4.20: Increase in Bulk Hardness Comparison (pure Copper)

imum increase in hardness for 'rubber assisted' and 'without rubber' forming is 141 BHN and 179 BHN respectively. It can be inferred that rubber based process generated less stress in the component.

Microstructure Analysis and Comparison

Similar to previous case microstructure analysis is also carried out to study the grain distortion. Samples are prepared using the 10mm width of the component along the profile. The representation of the sample is shown in figure 4.21. The samples are prepared as per ASTM E3-11 [67] standard. The analysis is carried to study the variation in microstructure size and its distribution. The samples are shown in figure 4.22. The microstructure grain analysis was carried out as per ASTM E112 [68].

The microstructure was captured at 4 locations in both the components as shown in figure 4.23. The microstructures at all the 4 locations for rubber-assisted process is presented in figure 4.24. It is clearly evident that all 4 microstructures are more or less same and there is no significant pattern of grain distortion. It can be inferred that the strain induced in the component is more or less uniform.

Figure 4.25 shows the microstructures for "Without Rubber Process". The grain

boundaries are missing at many places, which clearly indicates that there is severe grain distortion in this process. Hence, there is non-uniform progression of strain.

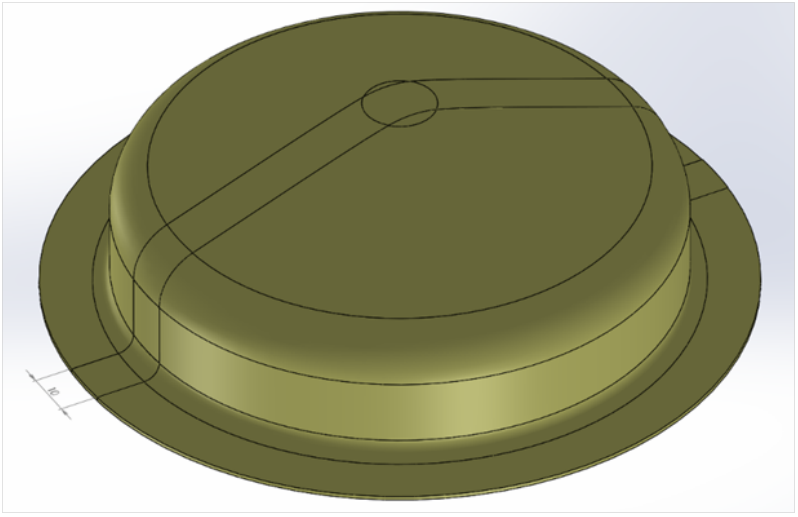

Figure 4.21: 3D model for Sample location (pure Copper)

The comparison of microstructures at location 1, 2 & 3 is presented in figure 4.26. The flow lines are very dense & No clear Grain boundary visible in “without rubber process". Also the grains are slightly more distorted in this case. Whereas “Rubber assisted Process" has very minimal grain distortion which indicate that deformation in this case is significantly less.

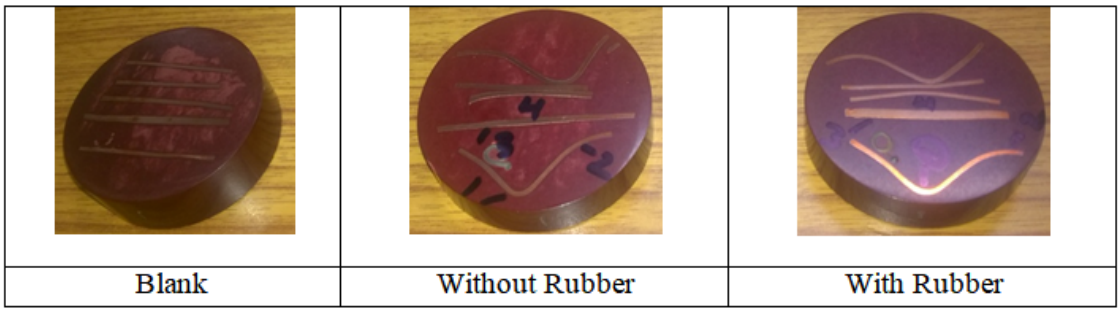

Figure 4.22: Samples for Micro-hardness (pure Copper)

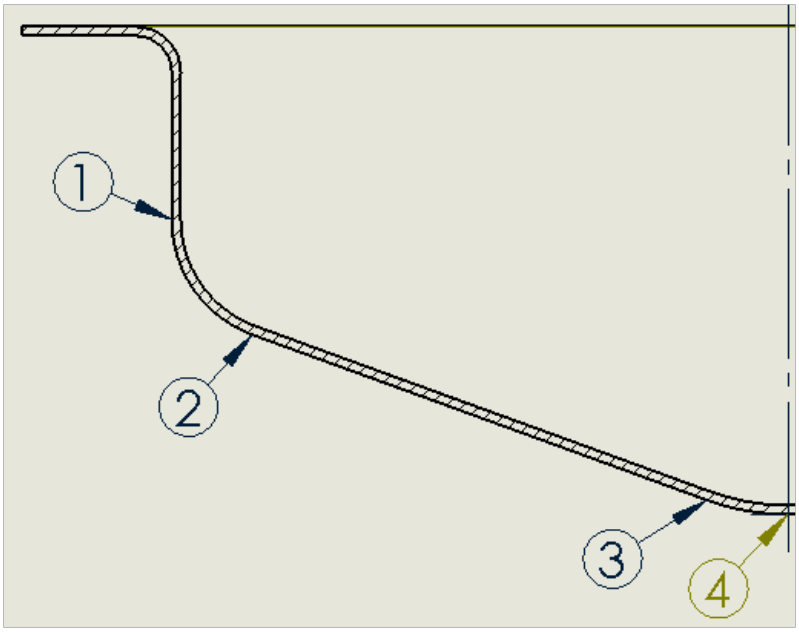

Figure 4.23: Locations for Microstructure analysis (pure Copper)

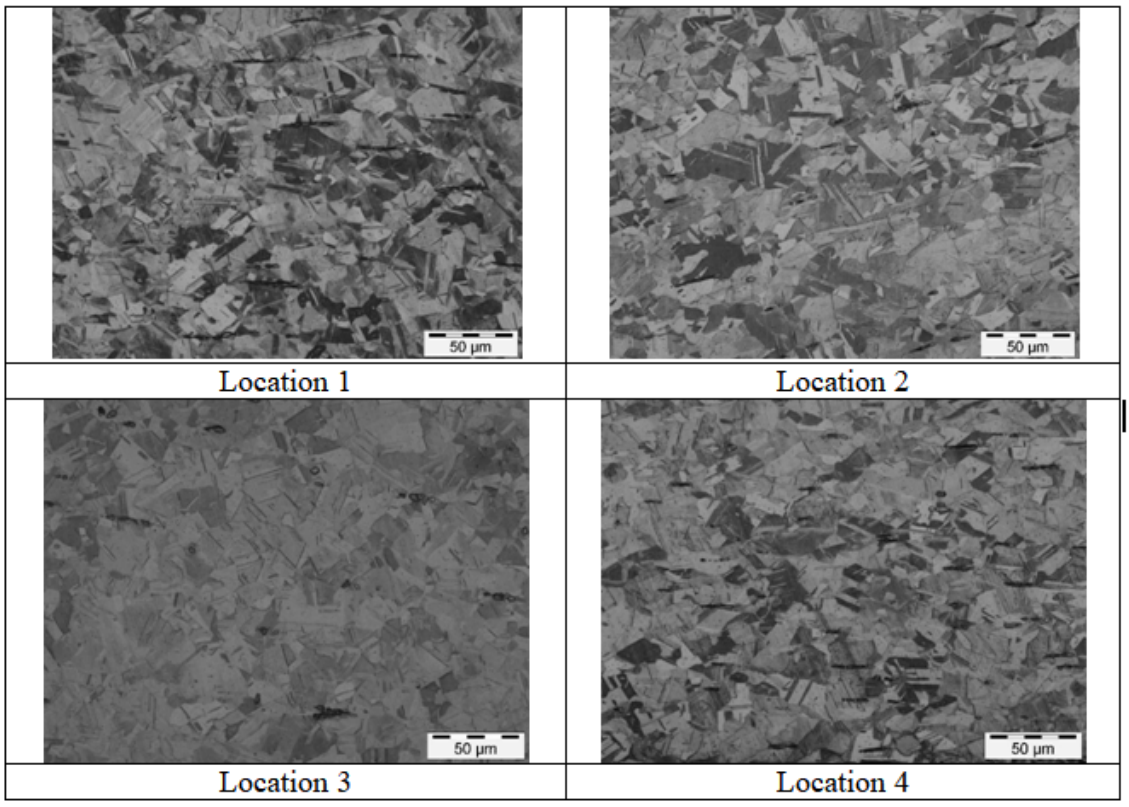

Figure 4.24: Microstructures (Rubber Assisted Process (pure Copper))

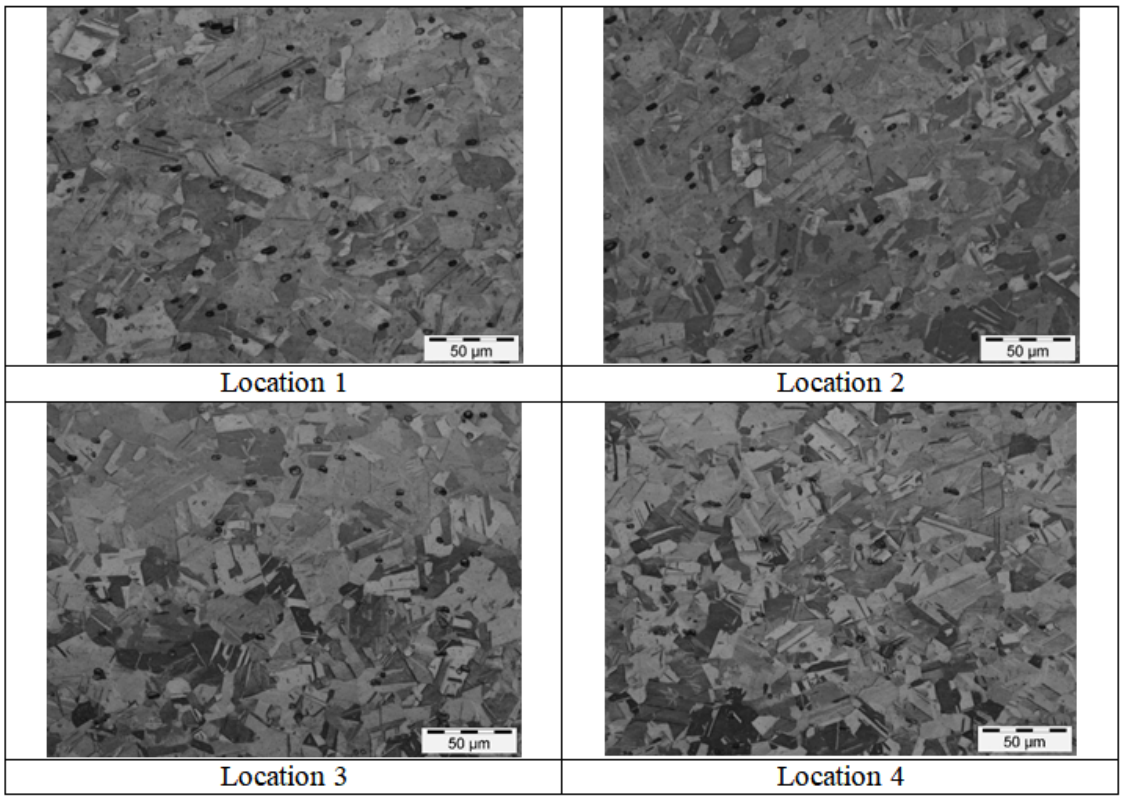

Figure 4.25: Microstructures (Without Rubber Process (pure Copper))

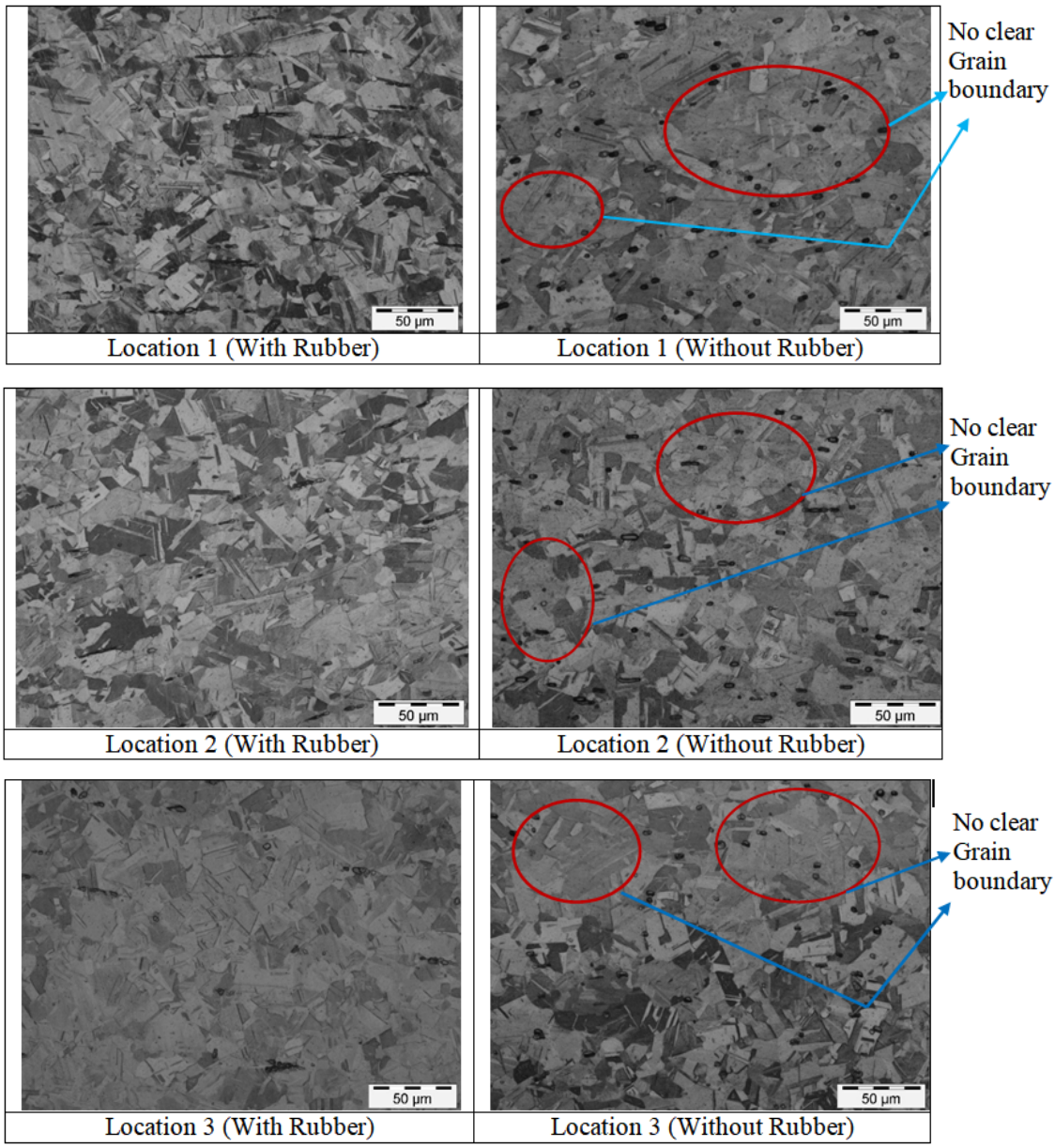

Figure 4.26: Comparison of Microstructures (pure Copper)

4.3 For height to diameter ratio greater than 0.5 (Deep Drawing)

4.3.1 Study for Cone made of Pure Copper

Die Design and Experiment

It is decided to evaluate the process for complex shapes having higher Shape Factor. Conical shapes are one of those shapes which are very difficult to deep drawn. It usually needs multiple stages to get formed without fracture. With this aim, the dies are fabricated to suit Rubber-assisted forming. The conical component is made up of Pure Copper (>99% Purity). The experiments are conducted for both “With Rubber Support" and “Without Rubber Support" processes. The wall thickness of the component is measured using micrometer having least count of 50 microns.

In this setup punch angle is 84^o & tip radius is 11 mm. Blank material is Pure Copper & thickness is 2 mm. Material for Die, Die Block and Blank Holder is Mild Steel. Natural Rubber of 3 mm thickness has been used to evaluate and compare the formability of rubber assisted process with conventional forming. The CAD Model of assembly is shown in Figure 4.27. The grid of ϕ 5mm is marked to study Major and Minor strain of the component. The component has been formed first “with rubber" and then “Without Rubber". The variation in wall thickness is presented in next section. Figure 4.28 shows the actual hardware of die assembly. The assembly setup on press machine is shown in figure 4.29.

Formability study using percentage thinning as parameter

The failure took place in initial trials because forming was done in hardened condition. Subsequently, annealing of Copper blanks has been carried out at 500 ^{o}C [69] to relieve internal stresses. The formed components are shown in figure 4.30. Total 5 points are marked on both component by permanent marker. The thickness at each point is measured by Micrometer (Least count 10μ) then take average of all

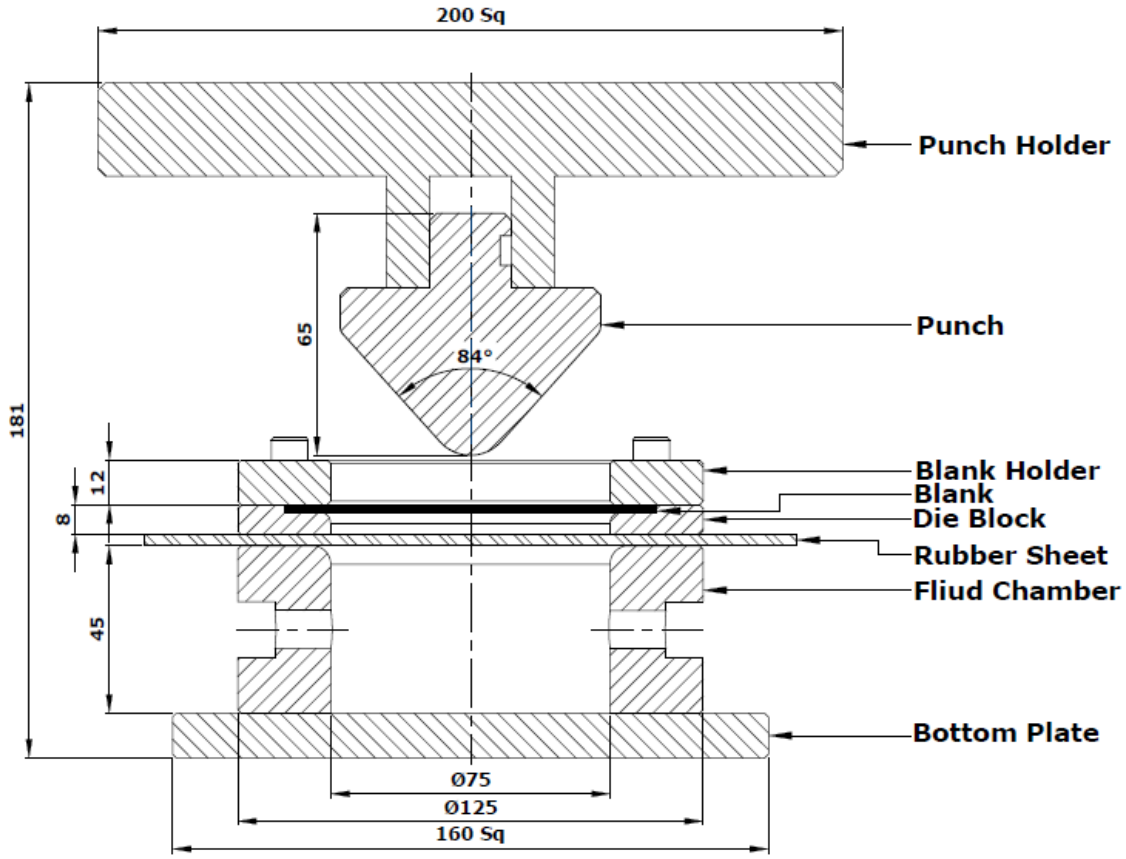

Figure 4.27: Die Assembly for Conical Component

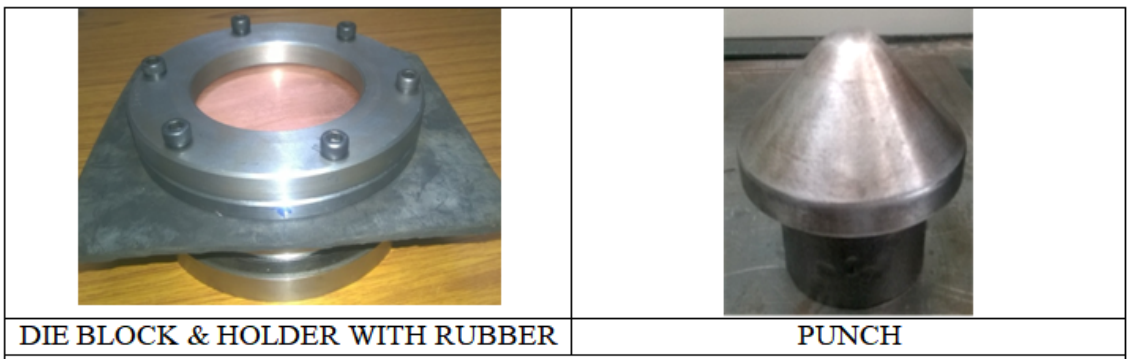

Figure 4.28: Die assembly and Punch for forming of Conical Shape

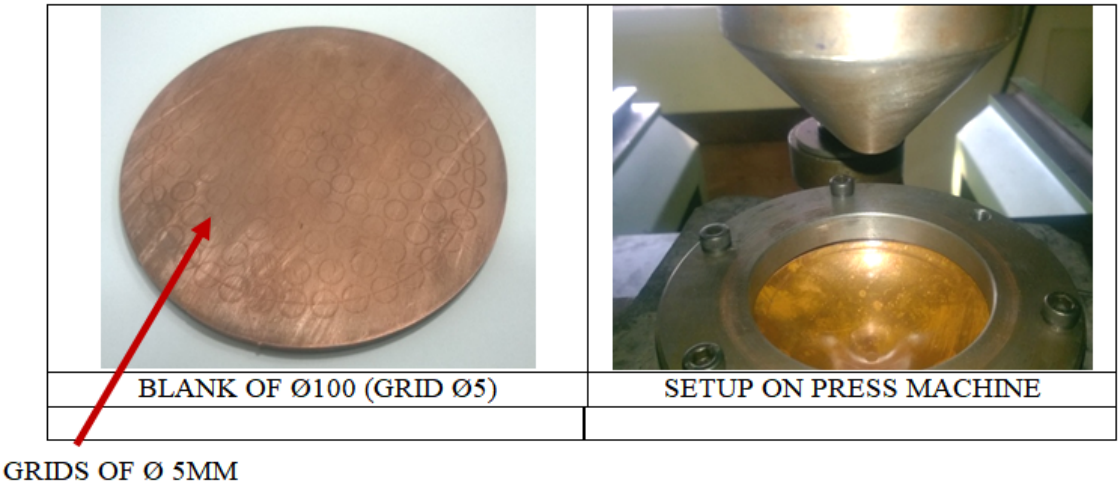

Figure 4.29: Deep Drawing Setup On Press Machine

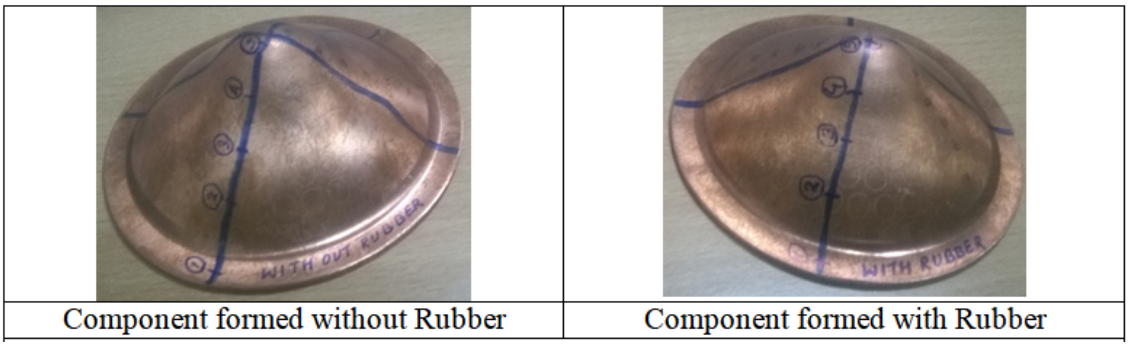

Figure 4.30: Components formed using both Processes

Station	With Rubber	With Out Rubber
1	2.03	2.02
2	1.955	1.935
3	1.885	1.825
4	1.61	1.3
5	1.6	1.5
Thickness Value At 5 Location		

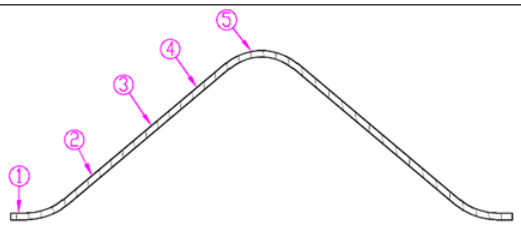

Section View Of Pure Copper Cone

Figure 4.31: Comparison Of Thickness for Both Processes

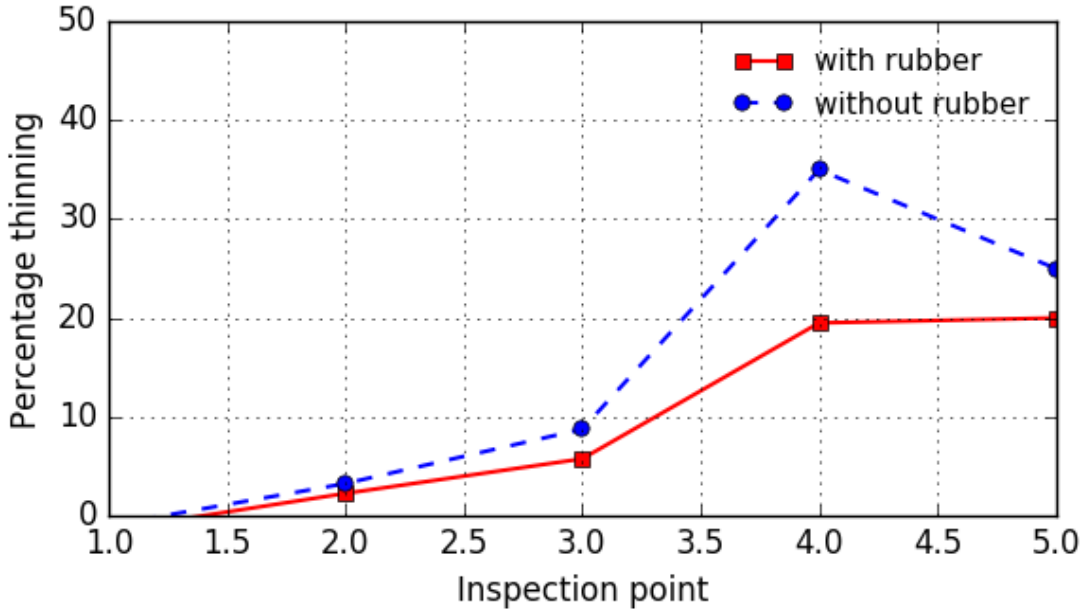

Figure 4.32: Thickness Comparison at 5 Location

same level points. All points shown in figure 4.31.

Vasco Manuel [70] in this thesis has pointed out that the zones of Bend and Re-bend is major zone of Failure and bottom of Component never undergo fracture. Hence, failure is expected not at the bottom but just above the bottom which is zone of bend and re-bend. Figure 4.32 shows the average thickness of components at 5 locations. As explained above, the location 4 is most critical for failure evaluation. At Point 4, the average thickness is 1.6mm in Rubber assisted process whereas it reduced to 1.3 mm in case of “Without Rubber" process. Hence there is 15% more thinning in 2nd case. It can be safely concluded that rubber assisted process has resulted in better strain distribution and delayed the localized necking during forming.

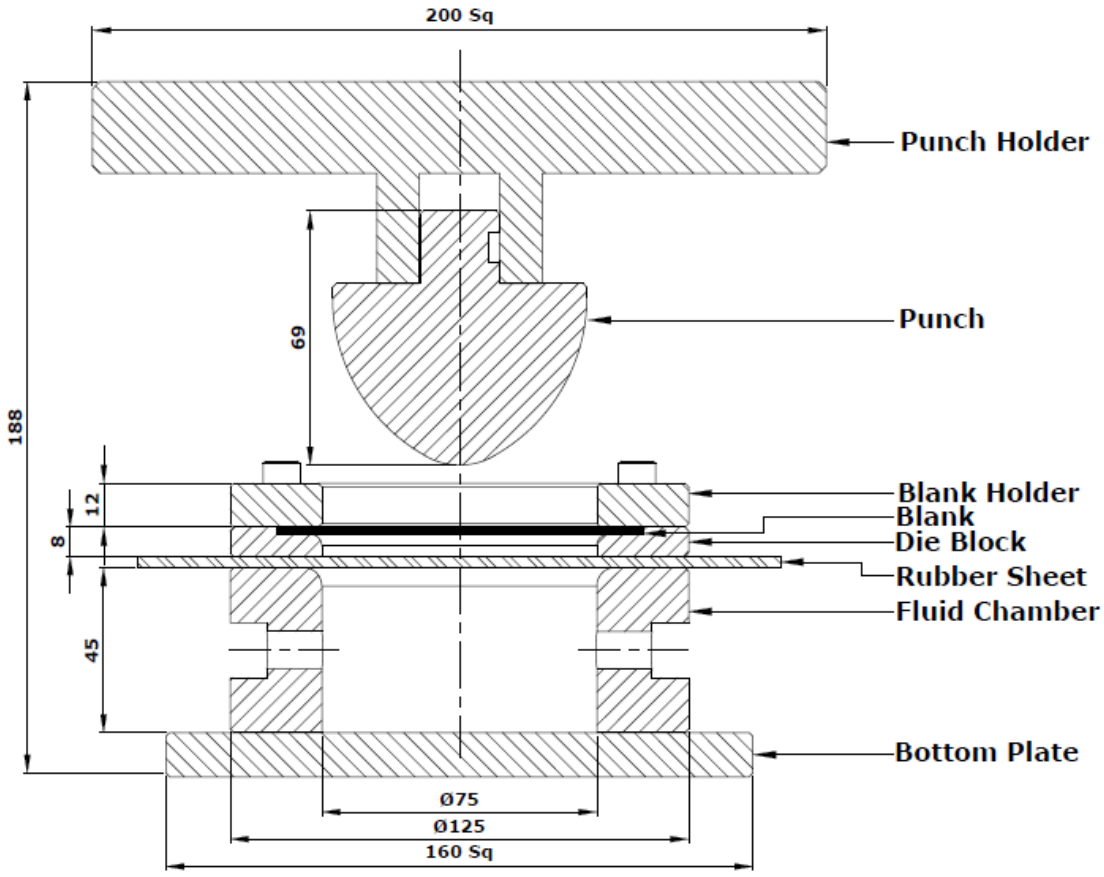

Figure 4.33: Die Assembly for Hemispherical shape Rubber-based deep drawing process

4.3.2 Study for Hemispherical Cup made of Pure Copper

Die Design and Experiment

In this case, conical punch is replaced with Hemispherical punch having diameter of 70 mm. Other die design remains unchanged. Figure 4.33 shows the die assembly for this experiment.

Formability study using percentage thinning as parameter

An experiment is performed to determine the formability of hemispherical copper cup in rubber assisted forming with natural rubber. The blank is made up of pure copper having initial thickness of 2mm. The hemispherical cup is drawn using both with rubber and without rubber processes. The thickness of rubber at various cross-section are measured at two section along the height of the cup. The details of percentage thinning is presented in table 4.3 and table 4.4 across X and Y section.

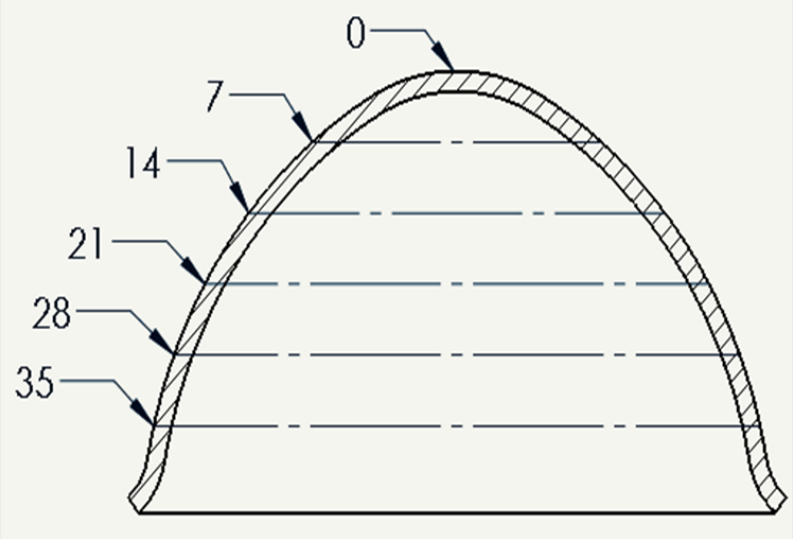

Figure 4.34: CAD model of Hemispherical Cone

Table 4.3: Thickness and percentage thinning in X-section

Height (mm)	**Thickness (mm)**		**Percentage of Thinning**	
	Without Rubber	**With Rubber**	**Without Rubber**	**With Rubber**
0	1.75	1.77	11.5	11.5
7	1.65	1.71	17.5	14.5
14	1.67	1.73	16.5	13.5
21	1.8	1.85	10	7.5
28	1.91	1.93	4.5	3.5
35	1.96	2	2	0

The comparative percentage thinning plots are shown in figures 4.35 and 4.36.

Table 4.3 shows thickness and percentage thinning along 'X' section. It indicates that at the depth of 14 mm, percentage thinning in rubber assisted forming and without rubber forming is 13.5 and 17.5 respectively. Similarly, along Y-section as shown in table 4.4, the maximum difference in percentage thinning is observed at the depth of 21 mm. The values are 10% and 14% in rubber asssited and without rubber forming process respectively. Therefore, it can be inferred that there is 4% improvement in thinning for forming of hemispherical cup using rubber assisted forming.

Table 4.4: Thickness and percentage thinning in Y-section

Height (mm)	**Thickness (mm)**		**Percentage of Thinning**	
	Without Rubber	**With Rubber**	**Without Rubber**	**With Rubber**
0	1.75	1.77	11.5	11.5
7	1.68	1.69	16	15.5
14	1.7	1.72	15	14
21	1.72	1.8	14	10
28	1.84	1.92	8	4
35	1.97	1.99	1.5	0.5

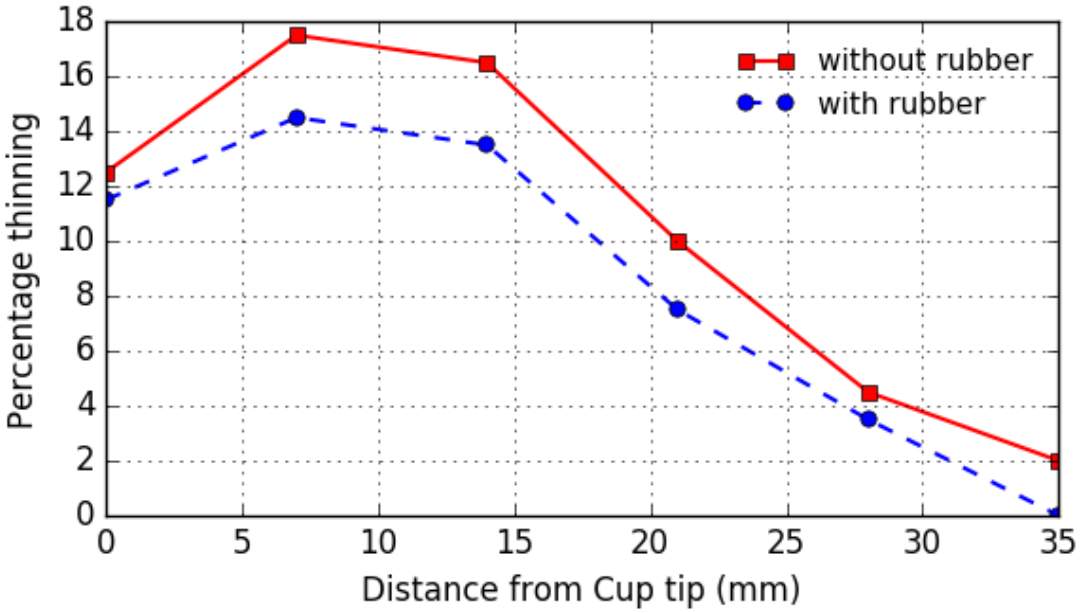

Figure 4.35: Comparative percentage thinning in X-section

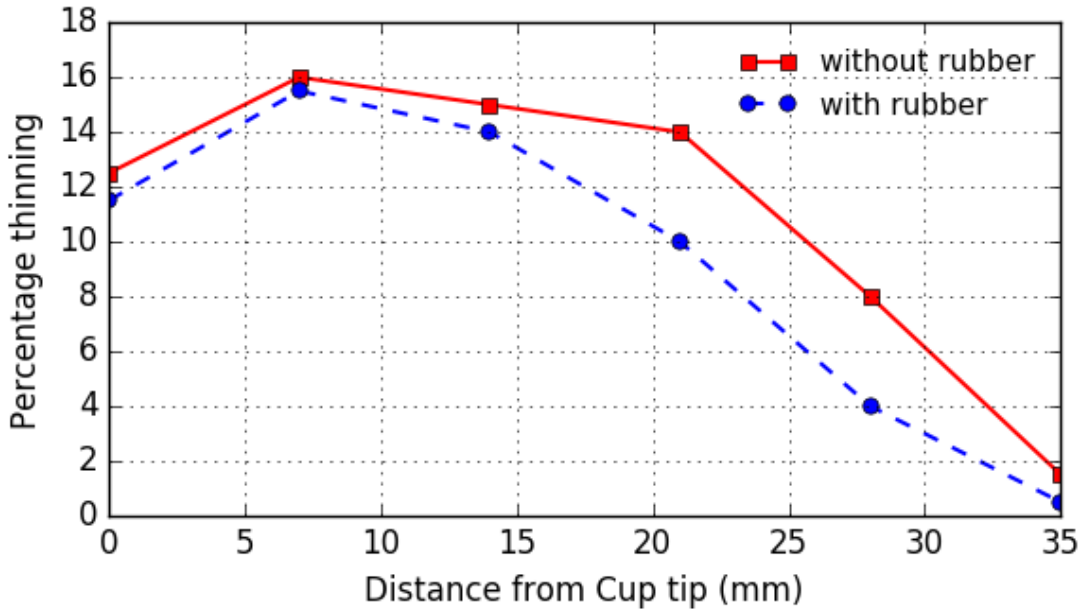

Figure 4.36: Comparative percentage thinning in Y-section

4.4 Formability study using Grid Method

4.4.1 Grid marking and measurement of Principal Strains

Circular grid analysis is a useful technique for diagnosing the causes of necking and fracture failures in manufacturing process [71, 72]. In sheet metal forming processes, the evaluation of strains by circular grid analysis is obtained through circular grid marking, which has been effectively used to solve the problems in metal forming. Before forming the sheet metal is marked with circular grids process. The grids can be of different shapes such as square arrays of contacting or closely spaced non-contacting circles or arrays of overlapping circles as shown in figure 4.37 [73]. With small closely spaced circles, it is possible to determine strain gradients accurately. During the forming operation, the grid pattern deforms with the material. The surface strains are measured from the deformed pattern by comparing its size to the original size of the grid pattern. Types of tools used in manual measurement include Dividers, Steel rule, Mylar tape and Traveling microscope [74]. The manual strain measurement methods are time-consuming and have low accuracy. As a result, automated surface strain measurement system has been developed [75]. This measured strains (major and minor) can be used to generate FLD for any sheet metal forming process.

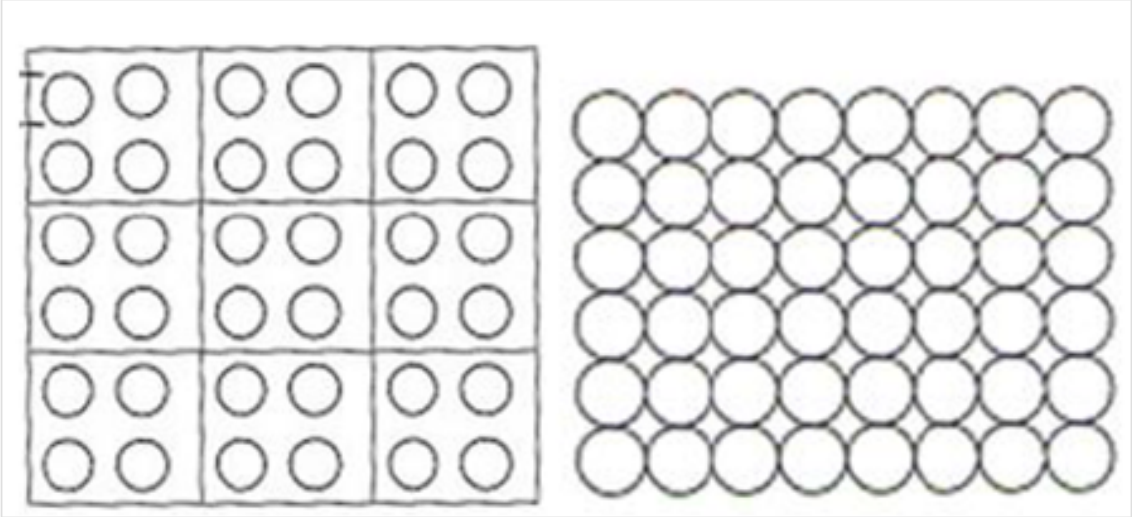

Figure 4.37: Pattern of circular grid [73]

Dr. R. Uday Kumar [73] carried out study on "Analysis of major strains and

minor strains in sheet metal forming". In sheet metal forming processes the evaluation of strains by circular grid analysis is obtained through circular grid marking, which has been effectively used to solve the problems in metal forming. M.Gerdooei and B.M. Dariani [76] worked on "Strain rate dependent FLD for sheet metals". FLD appears as one of the most applicable methods used for prediction of the instability in sheet metal forming. In this paper the effects of strain rate on FLD are analytically investigated over a wide range of strain rates 0.01/s - 500/s. L. Wang, and T.C. Lee [77] worked on "The effect of yield criteria on the forming limit curve prediction and the deep drawing process simulation". Theoretical FLC is calculated using swift model which considers three yield criteria Hill 48, Hill 90 and Hill 93. J. Slota and E. Spisak [78] also worked on "Comparison of the Forming limit diagram models for drawing quality steel sheets". In this a comparative investigation of three mathematical models (Mariciniak - Kuczynski model, hill swift model and Sing-Rao model) as well as an empirical model proposed by the North American Deep Drawing Research Group (NADDRG) has been carried out.

Thus the evaluation of formability in sheet metals has been completely established using FLD. In present work, Hill-swift model has used to evaluate the strains developed in the components and comparison is made to establish the advantages of rubber assisted forming.

4.4.2 Generation of theoretical Forming Limit Curve for Pure Copper

FLC developed by Dr. Stuart Keeler in 1960's is the most popularly used failure criterion for sheet metal forming. Keeler's methodology for generation of FLC has been described in section 2.1.1.

Hill's Swift Model

Hill's Swift is a generic model to calculate the theoretical FLC for any material. In present work, this model has been used to establish FLC for pure copper. These forming limit strains can be calculated by the Swift diffuse instability theory [79, 80, 81] and the Hill localized instability theory. The Swift diffuse criterion was derived

by assuming that there is a maximum loading force, Whereas Hill's localization criterion is obtained by assuming that there is maximum principal stress. Swift's and Hill's theories [82, 83, 84, 85, 86] are used to calculate the forming limit strains on the left and right side of the FLD respectively. The stress-strain relationship of sheets can be expressed by power law. The formability of a process is a function of number of factors such as material properties (e.g., Strain hardening coefficient, strain rate sensitivity, anisotropy ratio) and process parameters (e.g. strain rate, temperature).

According to Swift's and Hill's criterion, the formulae calculating the forming limit strains can be written as follows, with

$$\alpha = \frac{\sigma_2}{\sigma_1} \tag{4.1}$$

for ε_2<0:

$$\varepsilon_1 = \frac{1 + (1-\alpha) r_m}{1+\alpha} n \tag{4.2}$$

$$\varepsilon_2 = \frac{\alpha - (1-\alpha) r_m}{1+\alpha} n \tag{4.3}$$

for ε_2>0:

$$\varepsilon_1 = \frac{\left[1 + r_m\left(1-\alpha\right)\right]\left[1 - \frac{2r_m}{1+r}\alpha + \alpha^2\right]}{\left(1+\alpha\right)\left(1+r_m\right)\left[1 - \frac{1+4r_m+2{r_m}^2}{\left(1+r\right)^2}\alpha + \alpha^2\right]} n \tag{4.4}$$

$$\varepsilon_2 = \frac{\left[\left(1+r_m\right)\alpha - r_m\right]\left[1 - \frac{2r_m}{1+r}\alpha + \alpha^2\right]}{\left(1+\alpha\right)\left(1+r_m\right)\left[1 - \frac{1+4r_m+2{r_m}^2}{\left(1+r\right)^2}\alpha + \alpha^2\right]} n \tag{4.5}$$

The mechanical properties of 1mm copper sheet metal are as follows:

Strain hardening component (n) = 0.44

Plastic strain ratio (r) = 1

α = 0.1 to 0.9

α = 0.1, r = 1, n = 0.44

For $\epsilon_2 < 0$:

$$\varepsilon_1 = \frac{1 + (1-0.1)\,1}{1+0.1} 0.44 = 0.76$$

$$\varepsilon_2 = \frac{0.1 - (1 - 0.1)\,1}{1 + 0.1} 0.44 = -0.32$$

For $\epsilon_2 > 0$:

$$\varepsilon_1 = \frac{[1 + (1 - 0.1)\,1]\left[1 - \frac{2(1)}{1+r}0.1 + 0.1^2\right]}{(1 + 0.1)(1 + 1)\left[1 - \frac{1+4(1)+2(1)^2}{(1+1)^2}0.1 + 0.1^2\right]} 0.44 = 0.4122$$

$$\varepsilon_2 = \frac{[(1 + 1)\,0.1 - 1]\left[1 - \frac{2(1)}{1+r}0.1 + 0.1^2\right]}{(1 + 0.1)(1 + 1)\left[1 - \frac{1+4(1)+2(1)^2}{(1+1)^2}0.1 + 0.1^2\right]} 0.44 = -0.1735$$

Table 4.5: Theoretical strain values of copper From Hill's-Swift model

Stress ratio(α)	$\epsilon_2 < 0$		$\epsilon_2 > 0$	
	Major true strain	**Minor true strain**	**Major true strain**	**Minor true strain**
0.1	0.7600	-0.3200	0.4122	-0.1735
0.2	0.6600	-0.2200	0.4017	-0.1339
0.3	0.5750	-0.1353	0.4022	-0.0946
0.4	0.5028	-0.0600	0.4154	-0.0519
0.5	0.4400	0.0000	0.4400	0.0000
0.6	0.3850	0.0550	0.4719	0.0674
0.7	0.3364	0.1053	0.5015	0.1543
0.8	0.2933	0.1460	0.4738	0.2571
0.9	0.2547	0.1853	0.4930	0.3580

The stress ration (α) has been varied at regular interval of 0.1. It begins with α equals to 0.1 and ends at alpha equals to 0.9. Using equation 4.1 to 4.5, theoretical major and minor strains have been calculated. Table 4.5 shows the theoretical values of limiting major and minor strains for Pure Copper. The corresponding FLC is shown in figure 4.38.

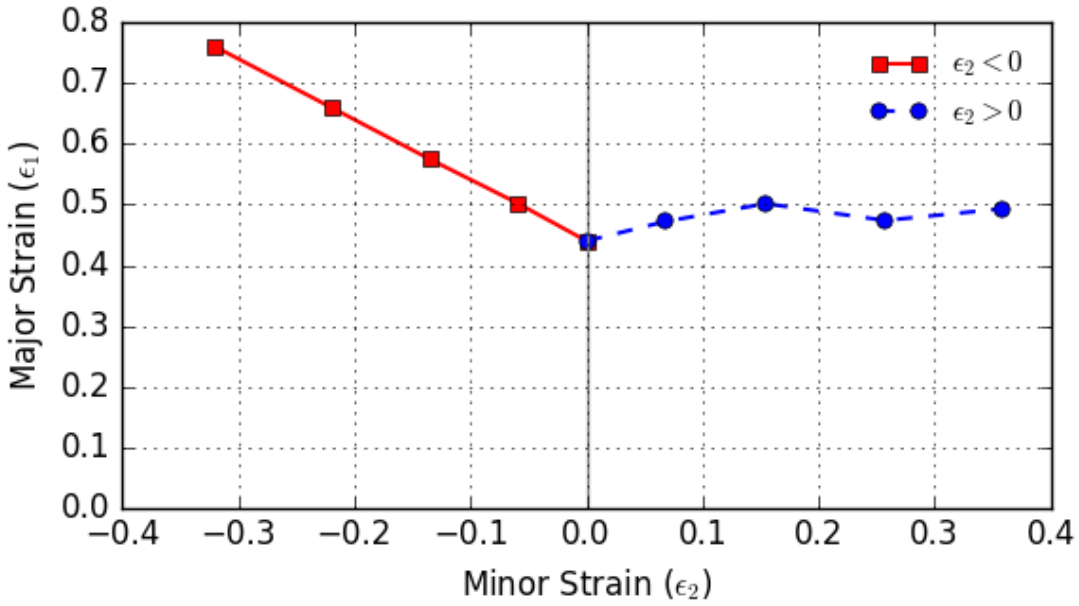

Figure 4.38: Theoretical FLC of Copper

4.4.3 Generation of Forming Limit Diagram from Measured Principal Strains

Grid marking has been done using chemical etching process. In this process first buffing is done to clean the entire surface of sheet metal. Here circular grids are used in grid analysis. First circle grids of diameter 7mm are marked on the surface of sheet metal and then the entire surface, other than the circle grids, is masked with Lacquer. Lacquer is the liquid solution which dries to a solid mask. Sheet metal is kept for one day at room temperature to dry that masked surface. Sheet metal is then immersed in Hcl solution for 22 minutes. Then, the sheet metal is removed from the solution and clean with water. Grid marking on blank is shown in figure 4.39.

The forming was carried out using 84^o cone. The forming set up is shown in figure 4.40. The formed components both with rubber and without rubber is shown in figure 4.41.

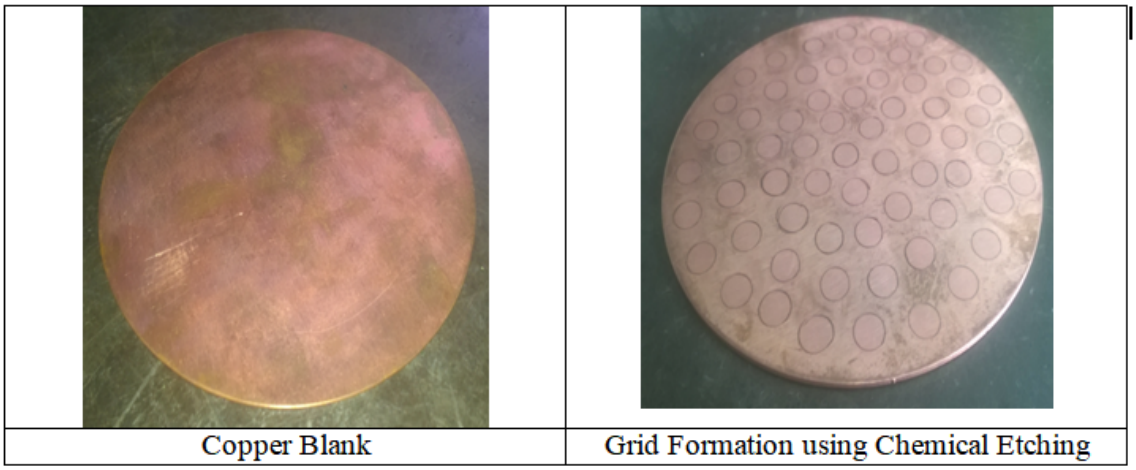

Figure 4.39: Grid marking using Chemical Analysis

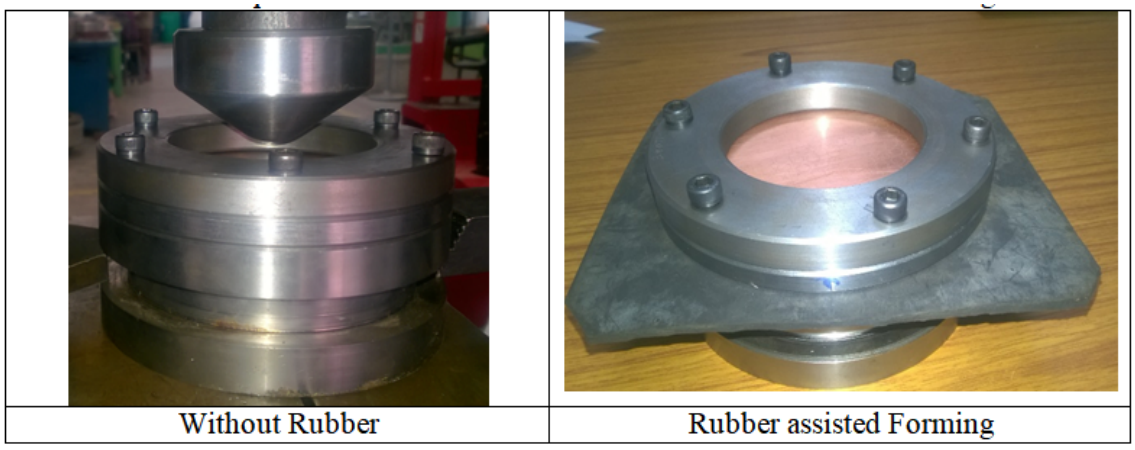

Figure 4.40: Experimental Set up for forming

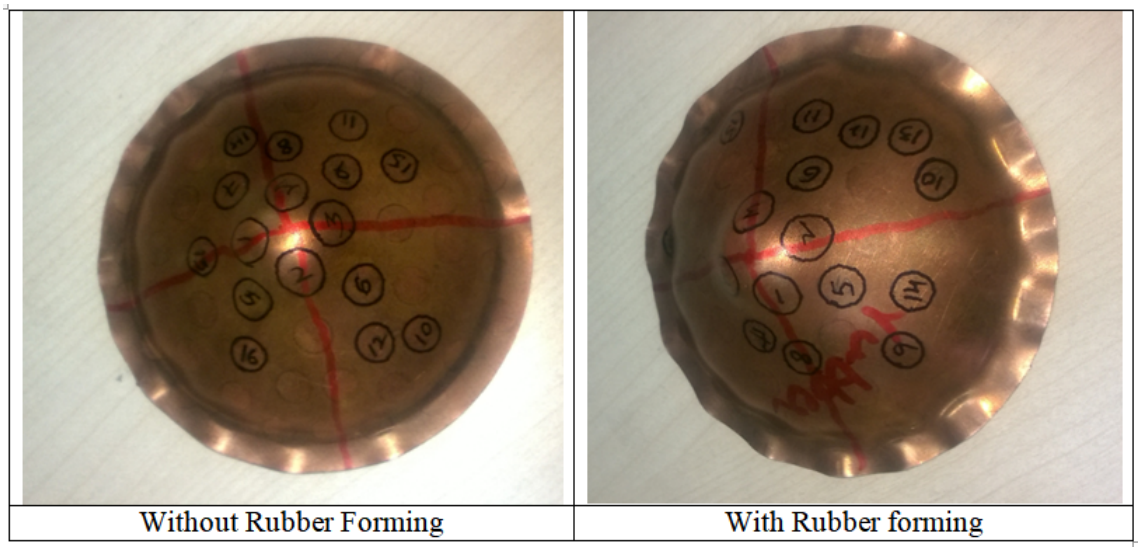

Figure 4.41: Formed cones and deformation of circle into ellipse

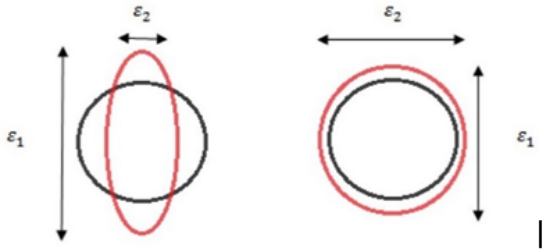

Circle grid before and after deformation black color circle shows the drawing area & red color stretched circle shows the stretching area.

Figure 4.42: Grid deformation before and after forming [72]

4.4.4 Comparison of FLD for both processes

To reduce experimentation through trial and error method which is both expensive and time-consuming, Keeler and Goodwin proposed grid strain analysis. The circle grid is the first method that has been done by Keeler (1964) and Goodwin (1968) to evaluate the FLD. The circle grid will show the deformation of sheet metal after the deep drawing process. The difference between diameter length of the circle before and after deformation can be recorded to evaluate the FLD [72]. The circle grid will deform into two types that is major strain and minor strain as shown in figure 4.42. Figure 4.43 is representing the deformation in grid circle under various forming conditions. As forming of Cone is a combination of stretching and deep drawing, the conditions as shown in point-A and point-C of Figure 4.43 are manifested in this experiment.

The black circle in figure 4.42 shows the circle grid before undergoing deformation, whereas the red circle shows the circle grid after deformation. The reading of both major and minor strain is recorded to evaluate the FLD which has been used to predict the formability of sheet metal.

The major and minor strain of the sheet can be calculated by using the formula

$$\text{Majorstrain}, \varepsilon_1 = \frac{D_{1,cg(major)} - D_{0,cg(major)}}{D_{0,cg(major)}} \tag{4.6}$$

$$\text{Minorstrain}, \varepsilon_2 = \frac{D_{1,cg(minor)} - D_{0,cg(minor)}}{D_{0,cg(minor)}} \tag{4.7}$$

Where,

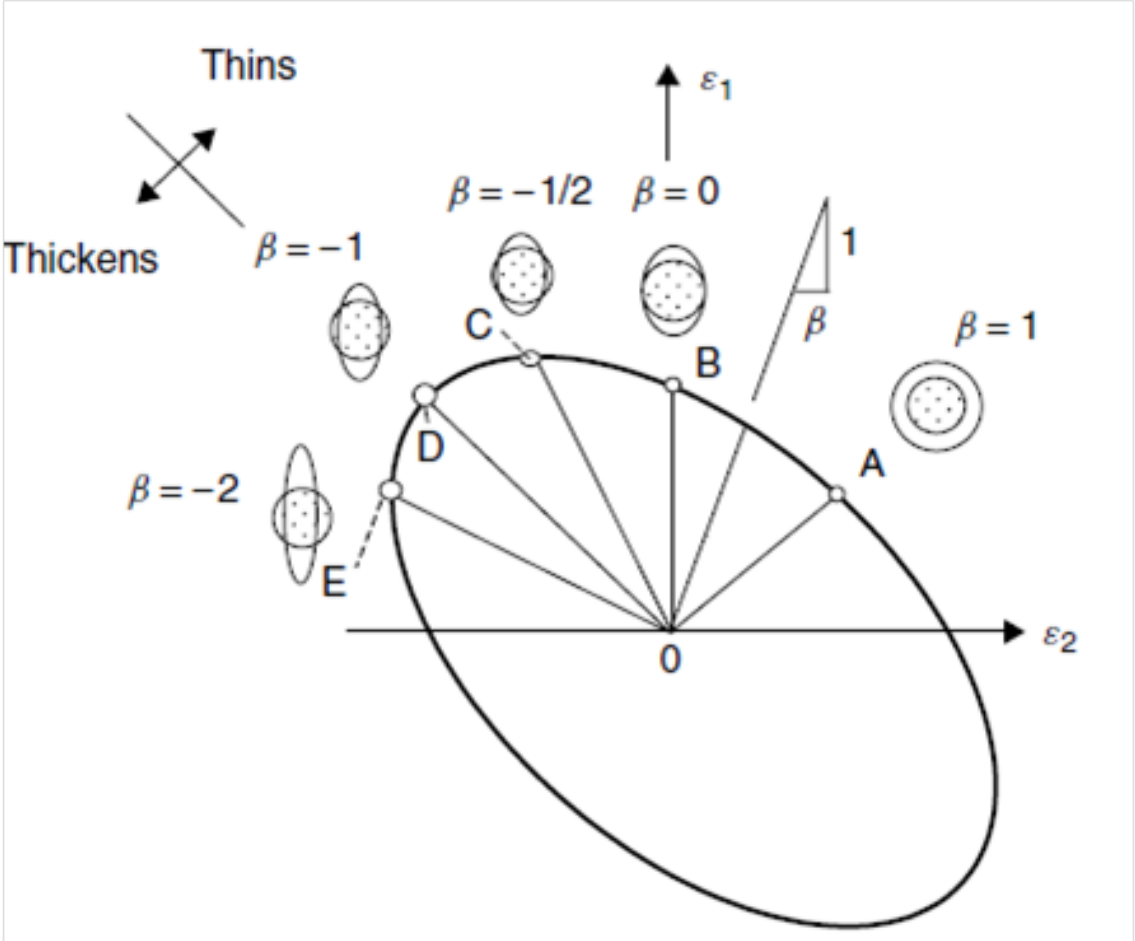

Figure 4.43: Deformation in circle under various forming conditions [87]

D_0 = Diameter of circle grid before deformation (mm)

D_1 = Diameter of circle grid after deformation (mm)

Strain measurment points and values

The strain values represented in a cad model for cone angle 84^o are listed in table 4.6. The plots of strain values against theoretical FLC is shown in figure 4.45. It is very much evident that rubber-assisted forming process generates less amount of strain.

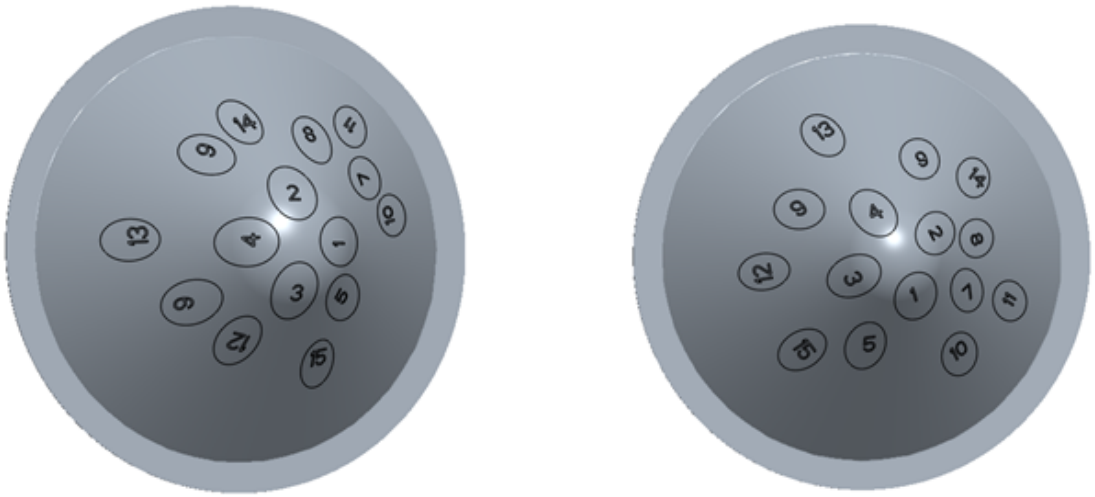

Figure 4.44: Strain measurement location

Table 4.6: The strain values - without rubber and with rubber

S. No	**with out rubber**		**with rubber**	
	Major True Strain (ϵ_1)	**Minor True Strain (ϵ_2)**	**Major True Strain (ϵ_1)**	**Minor True Strain (ϵ_2)**
1	0.2314	0.1514	0.1471	0.1314
2	0.2857	0.1628	0.2114	0.0114
3	0.2914	0.1200	0.1828	0.0285
4	0.2828	0.1428	0.1971	0.0114
5	0.1442	0.0143	0.1257	-0.0400
6	0.1457	0.0400	0.0742	-0.0314
7	0.1228	0.0171	0.1057	-0.0542
8	0.1428	0.0314	0.0885	-0.0686
9	0.1285	-0.0257	0.0857	-0.0229
10	0.1142	-0.0142	0.0829	-0.0114
11	0.1028	-0.0628	0.0943	-0.0485
12	0.0914	-0.0457	0.0542	-0.1085
13	0.0685	-0.0114	0.0514	-0.0657
14	0.0742	-0.0657	0.0457	-0.0800
15	0.0828	-0.1085	0.0828	-0.0628

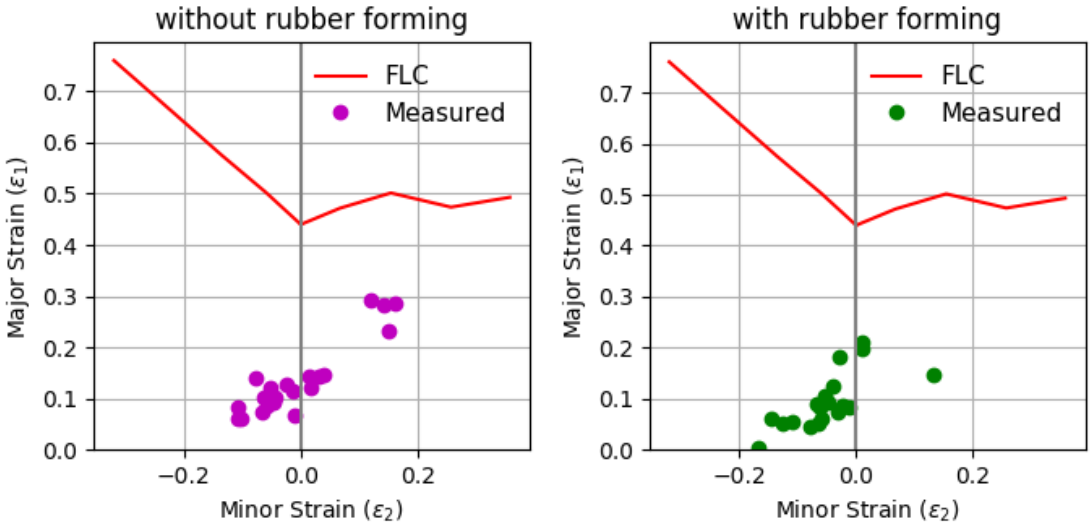

Figure 4.45: Comparison of FLD Plots

Figure 4.45 shows the comparison between the theoretical predictions based model and experimental FLD for copper sheets. The theoretical FLD is plotted from the values in Figure 4.38. The predictions by Hill-Swift model based on Hollomon's equation seems to be good to predict the forming behavior of copper sheet theoretically. The plot is generated with minor strain along X axis and Major strain along Y axis. As discussed in section 4.4.2, the minor strains can be both positive and negative depending on the mode of forming i.e stretching or deep drawing. The left hand side of the plot indicates drawing zone whereas right hand side indicates the stretching zone. The generation of theoretical FLC has been discussed in section 4.4.2. The same FLC of copper has been used in both cases. FLC indicates the fracture limit of the given material. Any major strain for a given minor strain should not cross the FLC line. The closer the major strain to FLC, the earlier will be the fracture. The plot of âĂŸwithout rubber formingâĂŹ and âĂŸwith rubber formingâĂŹ processes are shown in left hand side and right hand side of Figure 4.45. The plots have been generated using data given in table 4.6. The major strain values are ranging from 0.06 to 0.28 in 1^{st} case whereas from 0.04 to 0.21 in 2^{nd} case.

Usually, the points lying on the right hand side (RHs) of FLD are indicative of fracture. Hence, the critical values on the RHS of the plot are considered for comparison. It can be inferred that the major strain value (0.29) in case of "without rubber" are very close to the limiting value of FLC, whereas major strain value in

case of “with rubber forming" is only 0.18. Hence, Rubber assisted process improves the overall formability of the component. Also, as component has not failed, it indicates that theoretical FLC curve generated using Hill's Swift model is very much suitable for Copper material.

4.5 Effect of Rubber type on the Formability of Hemispherical Cup

4.5.1 Experimental Plan

Another experiment is performed to determine the formability of hemispherical copper cup in rubber assisted forming with natural rubber, silicon rubber and B-nitrile rubber. Figure 4.33 shows a schematic diagram of the experimental setup used in this study. The experiment has been carried out on a hydraulic press machine. The die clamped to the base and punch is placed at the top platen of the press machine. The copper sheet is placed on the upper surface of the die. The copper sheet is flat and is formed in hemispherical part as of the shape of punch. Below the die block the rubber sheet is placed, the sheet metal and rubber are pressed together by the punch. The hydrostatic compressive stress is generated by deformed rubber which can contribute towards improving formability. The elastomer incompressibility is exploited by deforming at constant volume as it exerts a hydrostatic pressure on the sheet metal. The blank holder is held tightly by C-clamps so that it presses the sheet firmly. Figure 4.46 shows the different hemispherical cup formed under Natural, Nitrile and Silicone rubber diaphragm.

4.5.2 Comparison of percentage thickness variation in radial direction

Deghani and Salimi [88] carried out measurement of thickness variation to predict the formability of material. In present work also, the percentage of thinning is used as a parameter to measure formability.

Table 4.7 and 4.8 shows the comparison of thickness variation and percentage of

Hemispherical cup formed by Natural rubber

Hemispherical cup formed by Nitrile rubber

Hemispherical cup formed by Silicon rubber

Figure 4.46: Hemispherical Cups formed with assistance of Rubbers

Table 4.7: Comparative thickness variation in X and Y section

S.No	Distance (mm)	Thickness variation (mm)		
		Natural	Nitrile	silicon
1	0	1.85	1.83	1.84
2	2.5	1.71	1.71	1.71
3	7.5	1.78	1.76	1.77
4	13	1.87	1.88	1.91
5	18.5	1.95	1.93	1.96
6	24.5	2.02	1.99	2.01
7	32	2.13	2.1	2.12

Thickness variation of hemispherical cup with different rubbers in X-section

S.No	Distance (mm)	Thickness variation (mm)		
		Natural	Nitrile	silicon
1	0	1.85	1.83	1.84
2	2.5	1.71	1.71	1.73
3	7.5	1.77	1.77	1.79
4	13	1.89	1.88	1.91
5	18.5	1.96	1.93	1.95
6	24.5	2	1.99	2.01
7	32	2.12	2.11	2.13

Thickness variation of hemispherical cup with different rubbers in X-section

Table 4.8: Comparative percentage thickness variation in X and Y section

S.No	Distance (mm)	Percentage of thinning (%)		
		Natural	Nitrile	silicon
1	0	7.5	8.5	8
2	2.5	14.5	14.5	14.5
3	7.5	11	12	11.5
4	13	6.5	6	4.5
5	18.5	2.5	3.5	2
6	24.5	-1	0.5	-0.5
7	32	-6.5	-5	-6

Percentage thickness variation of hemispherical cup with different rubbers in X-section

S.No	Distance (mm)	Percentage of thinning (%)		
		Natural	Nitrile	silicon
1	0	7.5	8.5	8
2	2.5	14.5	14.5	13.5
3	7.5	11.5	11.5	10.5
4	13	5.5	6	4.5
5	18.5	2	3.5	2.5
6	24.5	0	0.5	-0.5
7	32	-6	-5.5	-6.5

Percentage thickness variation of hemispherical cup with different rubbers in X-section

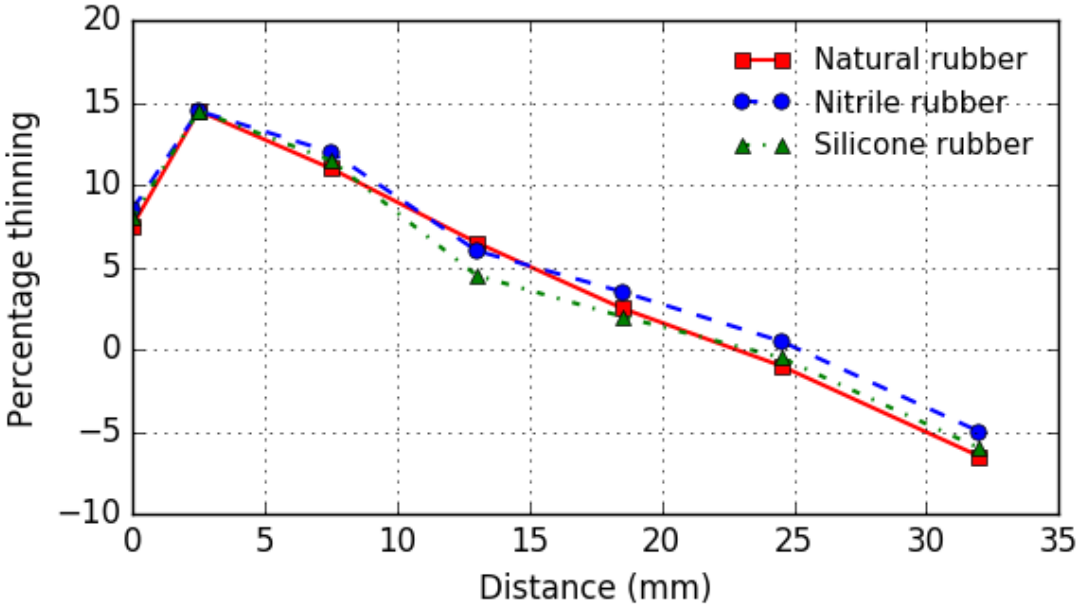

Figure 4.47: Comparative thickness variation in cup (X-section)

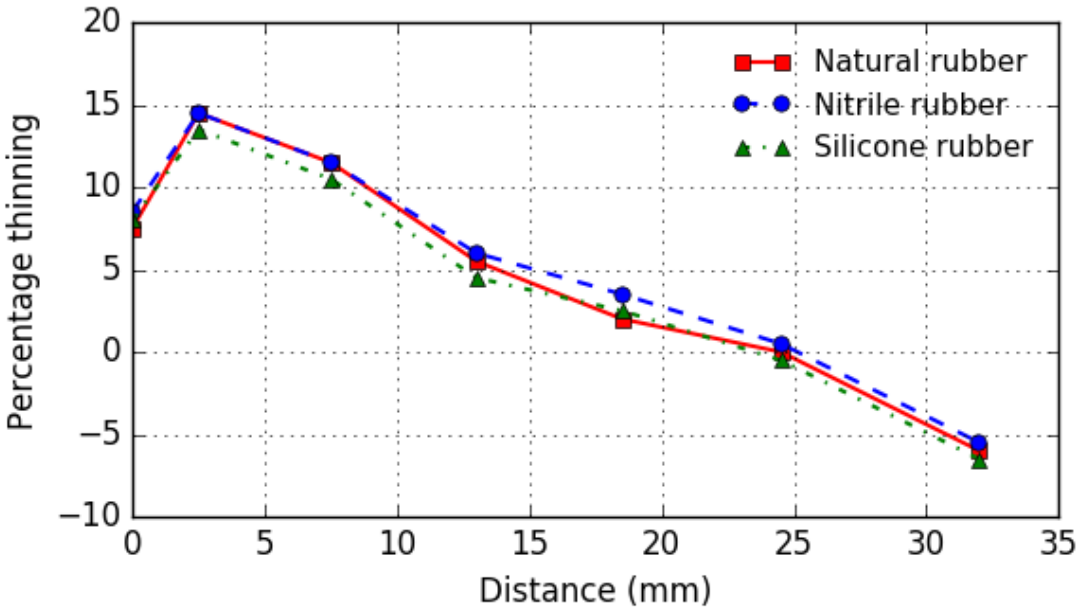

Figure 4.48: Comparative thickness variation in cup (Y-section)

thinning for hemispherical cup in rubber assisted forming with three rubbers (silicon rubber, natural rubber, and nitrile rubber). The hemispherical cup has been divided into two sections X and Y and the thickness has been measured according to the distance from the cup center in both the sections. This process is carried out for all three rubbers. Finally percentage of thinning in a hemispherical cup for three rubbers in both X and Y sections are compared.

It was assumed that as rubbers have different stress strain behavior, it may affect the formability of component. However, the obtained experimental results are new of its kind. As expected, the region of more thinning is nearest to the cup center. Figures 4.47 and 4.48 shows the comparison of the percentage of thinning between three rubbers (natural, silicon and nitrile rubbers). It can be observed that the percentage thinning of hemispherical cup is maximum near the center of the cup (2.5 mm) and it gradually decreases towards the cup flange. As expected, the thickening is observed in flange zone (32 mm). This trend of thickness variation is almost same for all three rubber variant. However, the numerical value of percentage thinning is equal at any cross-section of cup in all three cases. It can be inferred that as long as developed strain values during forming are within the limit of max permissible strain value, the effect of any rubber on formability would remain same.